ARC Far Side Impact Collaborative Research Program –

Task 5b & 6b: Model and Test Procedures Crash Tests and Sled Tests for the Far-side

Kennerly Digges

Editor

Pradeep Mohan

Chapter 1

Brian Alanso

Chapters 2, 3, 4 and 5

Joseph Cuadradro

Chapter 6

George Washington University

JUNE 2009

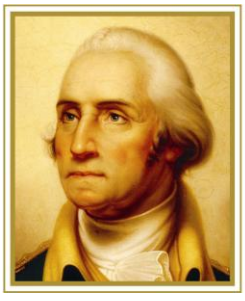

THE GEORGE WASHINGTON UNIVERSITY

WASHINGTON DC

Table of Contents

1. Crash Test Configurations for the Far-side Environment

1.1 Introduction:

In Task 1, the crash environment associated with injury producing far-side crashes was defined using US Accident data and confirmed from Australian data. The analysis indicated that for belted occupants with MAIS 3+ injuries, the 50% median crash severity was a lateral delta-V of 28 kph and an extent of damage of 3.6 as measured by the CDC scale [SAE Standard J224, Collision Deformation Classification]. The most frequent damage area for seriously injured belted occupants was the front 2/3 of the vehicle (42%), followed by the rear 2/3 (21%). The most frequent principal direction of force (PDOF) was 60º (60%), followed by 90º (24%). The head and chest were the most frequently injured body regions, each at about 40% [Gabler 2008]. The injuring contacts that most frequently caused chest injury were the struck-side interior (23.6%), the belt or buckle (21.4%) and the seat back (20.9%) [Fildes 2007].

This task applied finite element models of vehicles and barriers to determine the degree to which the NHTSA and IIHS barriers produced the extent of damage that would be expected in a far-side crash that is representative of the 50 percentile injury producing crash. The baseline test for this study was the impact of a full size pickup truck into the side of a Taurus. For a delta-V of 28 kph and a 90 degree impact with the occupant compartment, the extent of damage was approximately 3.6.

This test formed the basis for comparing the deformation produced by the NHTSA and IIHS barriers. Other crash conditions were conducted to determine the crash severity that produced deformation that was similar in extent to the 90 degree test.

1.2 FEM Model Simulations:

FE Model of the Ford Taurus was chosen as a representative mid-size sedan for this study. The model is one of the most detailed models developed at the National Crash Analysis Center. The model consists of 850K elements (Guerra, 2006). The FE model is used in this study as a target vehicle and the crush measures are taken at 4 different levels based on the US-LNCAP test protocol. The FE model of the Ford Taurus is shown in figure 1.

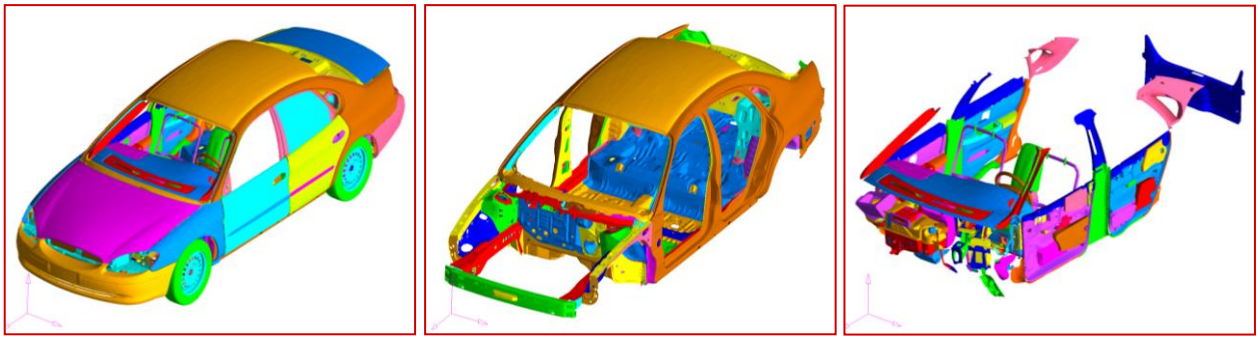

Figure 1: FE Model of the Ford Taurus

The US-LNCAP and the IIHS side impact barriers were used as the bullet vehicles in this study. Both of these barriers were recently developed at the National Crash Analysis Center (Kildare 2005). The barriers have been validated for the available load cell wall tests. The FE model of the US-LNCAP barrier along with the validation result is shown in figure 2. The load cell wall force from the FE model correlates well with the test data. The FE model of the IIHS side impact barrier along with the validation result is shown in figure 3. The load cell wall force from the FE model correlates well with the test data for the first 30 ms. Beyond 30 ms, the honeycomb compacts completely resulting in higher force level in the FE model. The actual crush of the barrier in the available tests into mid-size car shows that the barrier does not go into full compaction and the working limit would be within the crush observed in the first 30 ms of the load cell wall test.

The third bullet vehicle used was a GM C-1500 pick up truck.

Figure 2: FE Model of the US-LNCAP Barrier and the Load Cell Wall Force Comparison

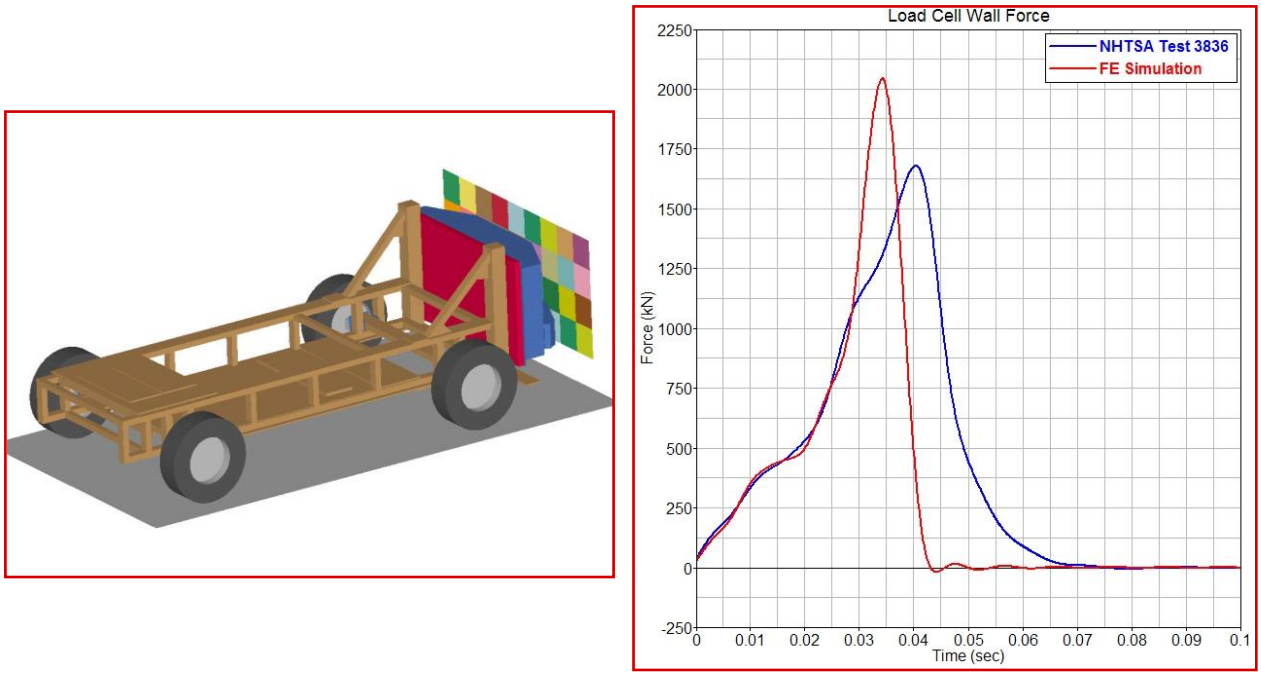

Figure 3: FE Model of the IIHS Side Impact Barrier and the Load Cell Wall Force Comparison

The five different impact configurations and the measured lateral delta-V for each of the configuration are shown in Figure 4. The first two configurations were based on the US-LNCAP and IIHS test protocols respectively. The remaining three impact configuration was with a GM C-1500 pickup truck. In the first case the impact point was at the mid of the front door and the impact angle was 60^0. The next case was set-up similar to the IIHS side impact protocol except that the bullet vehicle was a pick-up truck instead of the barrier. In the third case the impact point was at the front body hinge pillar.

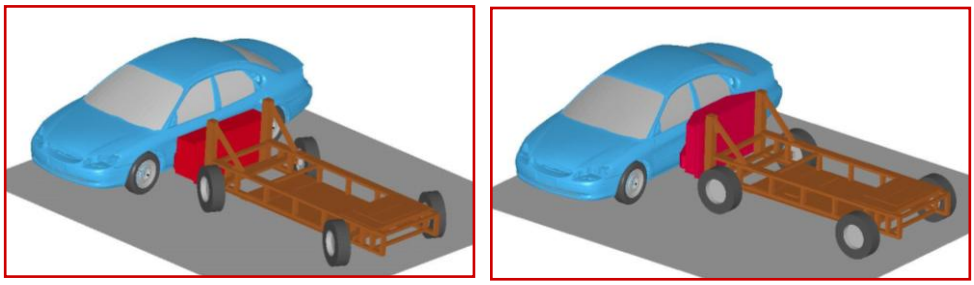

Delta V – 25.8 kph Delta V – 25.2 kph

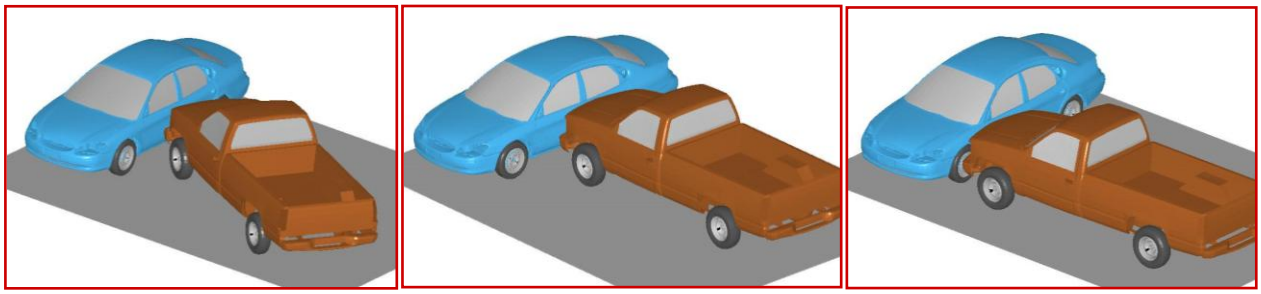

Delta V – 22.2 kph Delta V – 28.8 kph Delta V – 23.8 kph

Figure 4: Impact Configurations – NHTSA barrier; IIHS barrier, Pickup at 60°; Pickup at 90°; Pickup in Y-Damage configuration

The crush measures from the above impact configurations are shown in figures 5 through 7. The third impact configuration with the pick-up truck produces the max exterior crush at the windowsill. The extent of damage was about CDC 3.8. Except for the last impact configuration the other 4 cases produces similar crush characteristics. Based on these crush measures the pick-up truck impacting the mid of the front door produces the max exterior crush. The crush measures from the US-LNCAP simulation were compared to the test data available from NHTSA. The FE model yields a softer response compared to the test data. The model needs to be further validated and the front seat models needs to be included to obtain better correlation with the test data. Once the model is validated then the crush measures can be used as an input to MADYMO simulation to study the dummy kinematics with the intruding structure.

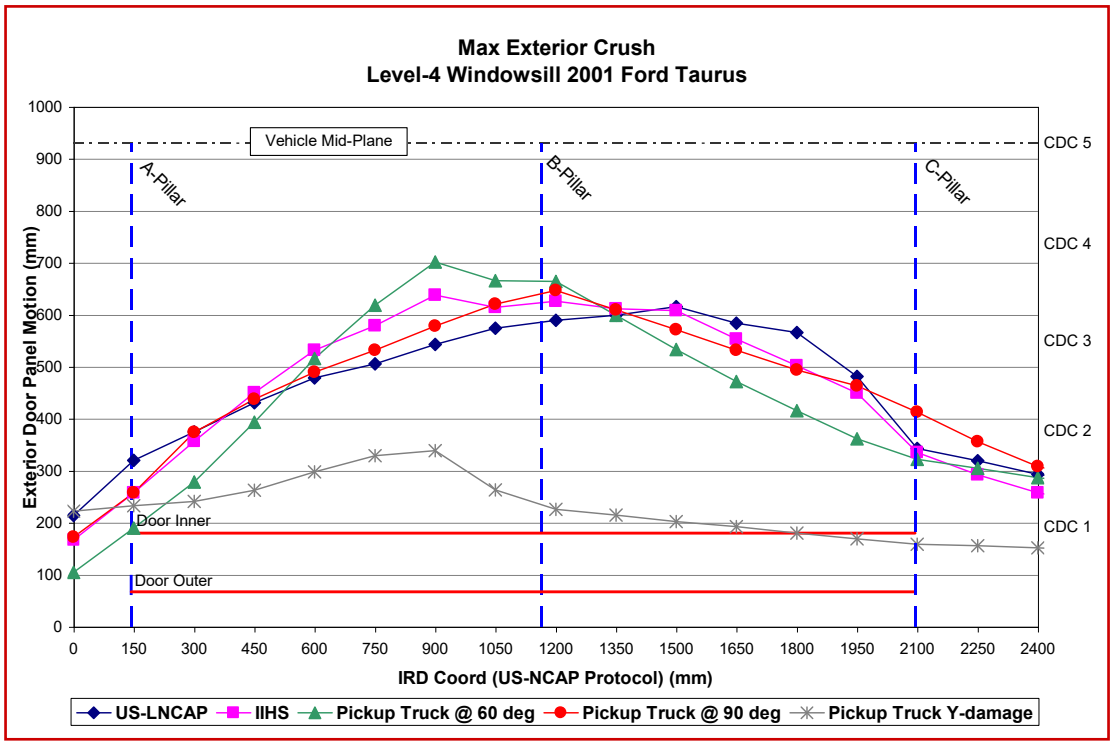

Figure 5: Max Crush at Windowsill

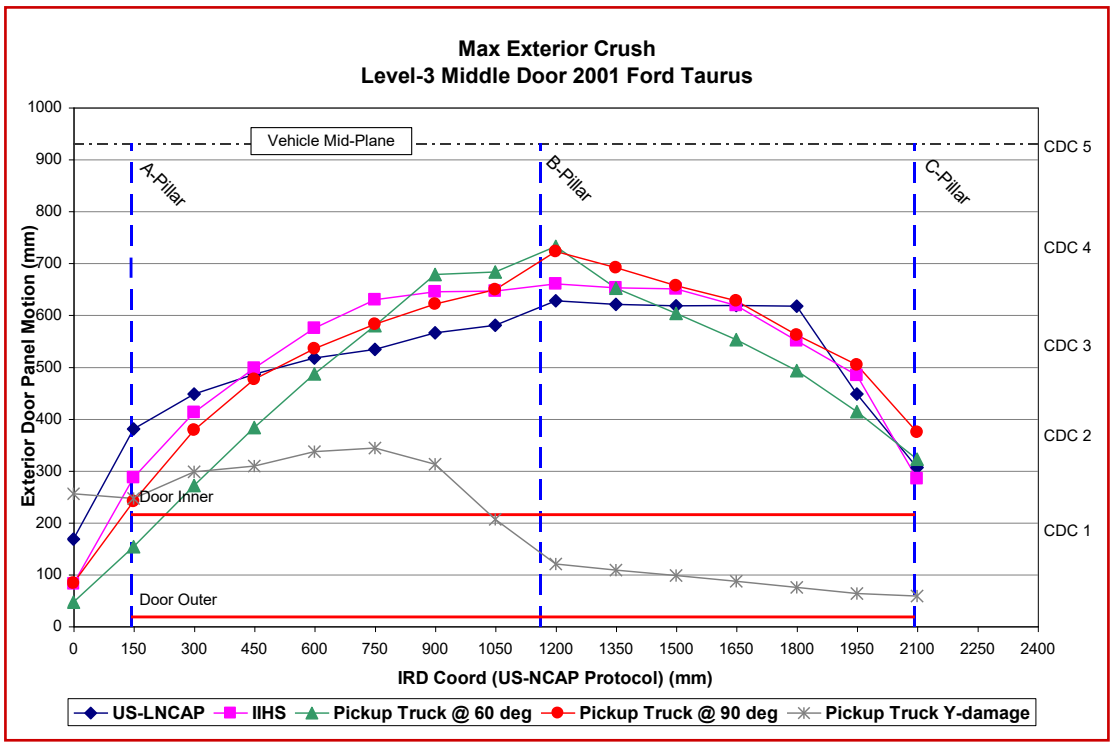

Figure 6: Max Crush at Mid-door

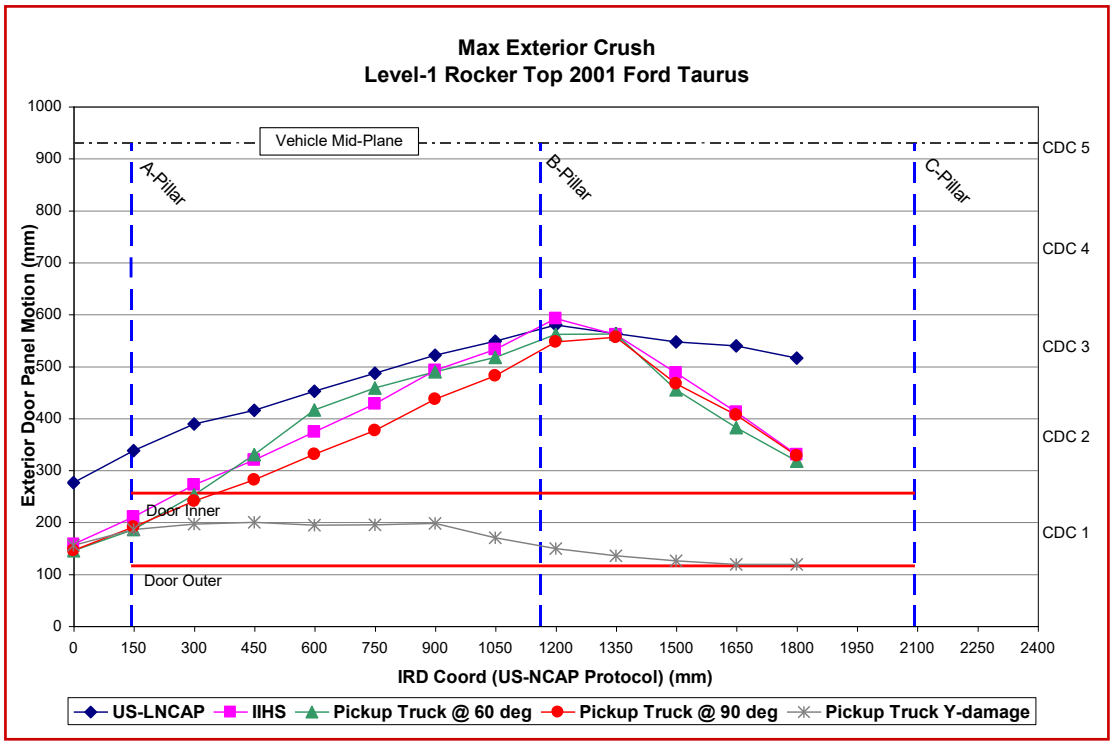

Figure 7: Max Crush at Rocker

1.3 IIHS Crash Test Deformations vs. Model Results

The IIHS database of side crash tests was examined to determine crush profiles of vehicles tested. The data on the following 12 vehicles were available:

Honda Accord, Nissan Altima, Toyota Camry, Subaru Forrester, Mitsubishi Galant, Saturn L series, Chevy Malibu, Mazda 6, Volvo S40, Saab 9-3, Hyundai Sonata, Dodge Stratus.

A plot of the average deformation at the mid level of the door for the 12 vehicles is shown in Figure 8 as the plot in blue. The average delta-V of these tests was 23.6 kph. The average CDC extent of deformation was 2.2. The pink plot shows the FEM simulation for a IIHS barrier impact with a Ford Taurus at a delta-V of 25.8 kph.

The higher deformation in the FEM simulation is partially due to the elastic component of deformation that is present in the FEM results but not in the IIHS test results. After the test there is a spring-back of the door structure. There may also be differences due to the higher delta-V for the FEM test. Finally, the model may not account for some of the structural interactions including seat and floorboard interactions.

Figure 9 provides two adjustments to the FEM model. The red curve adjusts the FEM deflection for spring-back. Scaling the FEM curve by a factor of 0.7 brings the FEM model close to the IIHS average deformation pattern..

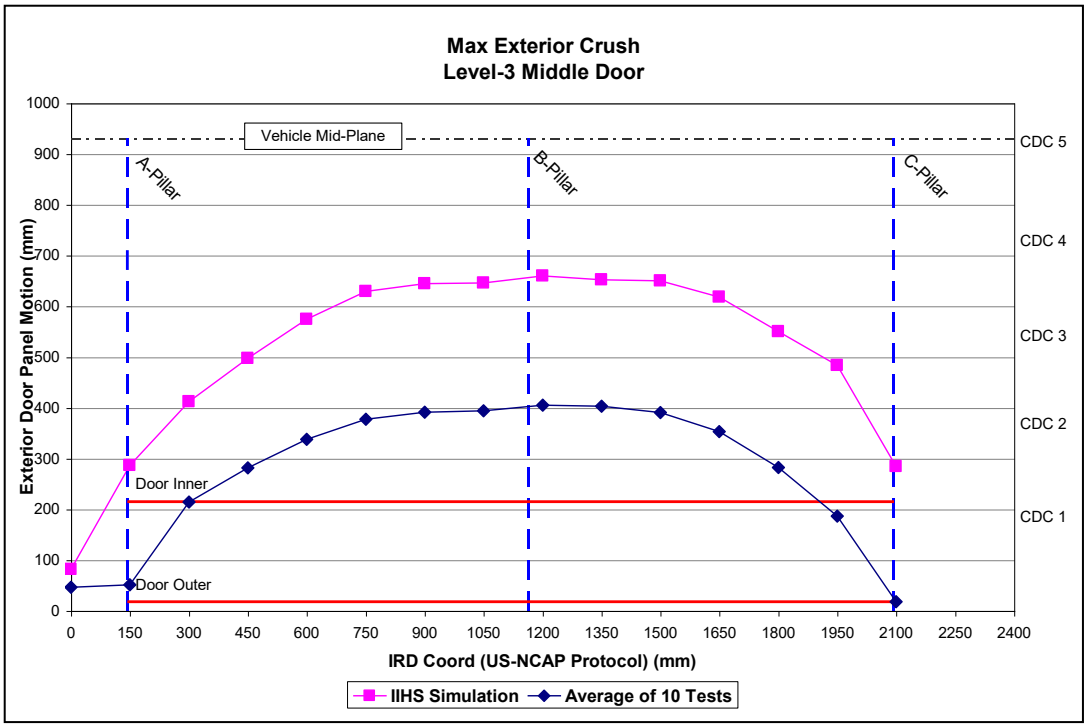

Figure 8. Side deformation – Average of 12 IIHS Tests with Delta-V of 23.6 kph and Predictions from FEM Model with a Delta-V of 25.6 kph

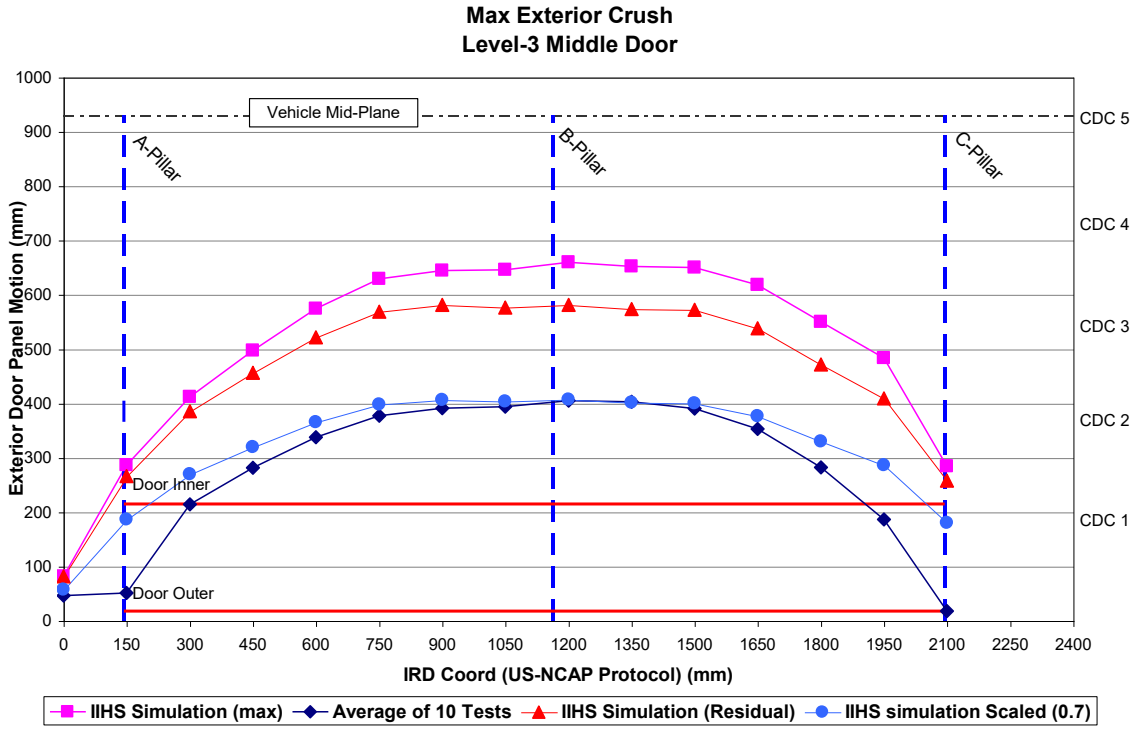

Figure 8. Side deformation – Average of 12 IIHS Tests with Delta-V of 23.6 kph and Predictions from FEM Model with a Delta-V of 25.6 kph; Adjustments to FEM model for Spring-back and Other

1.4 Discussion

Figure 9 shows a comparison of the residual deformation typical of IIHS tests and the deformation predicted by the Taurus model. The predicted shape of the deformation matches the test data. However, the extent of deformation predicted by the model is higher. This result suggests the need for further validation of the model to predict the extent of damage. However, the model is assumed to be useful in predicting the shape of the damage.

The shape of the damage predicted by the model for the IIHS test was generally similar in shape and extent to the damage produced by a pickup impacting the occupant compartment. Both the NCAP test and the Y damage test produced less damage to the front door than the IIHS test or the pickup impacts with the occupant compartment. This observation indicates that the IIHS barrier is the most suitable for simulating vehicle impacts to the front door of the occupant compartment.

As reported in Chapter 2, the average CDC extent of damage for far-side occupants who sustain AIS 3+ injuries is 3.6. The average CDC extent of damage produced in the IIHS tests plotted in Figure 9 is 2.0. This difference suggests that the far-side test aped should be higher than the near-side test speed used by IIHS.

The maximum deformation for the pickup impact was within 230 cm of the centerline of the Taurus. This produced an extent of damage of approximately 3.6. The Y-damage impact produced a lower extent of damage than that produced by the central impacts.

1.5 Conclusions

The Finite Element Models indicate that the IIHS barrier produced similar damage on a Taurus patterns to those produced by a full size pickup truck. The NHTSA barrier and the Y damage test produced less damage to the Taurus front door than the IIHS barrier.

The average CDC extent of damage produced in actual IIHS crash tests is considerably less that the average extent of damage to vehicles with far-side occupants injured at the AIS 3+ severity.

Further work is needed to validate the FEM model at the higher crash severities that cause serious injuries in far-side crashes.

1.6 References

Guerra, R.C., "A Refined Methodology for Vehicle Finite Element Modeling Incorporating Robust Capabilities, Fine Uniform Mesh, and Comprehensive Interior" A Thesis for the School of Engineering and Applied Science of The George Washington University, August 13, 2004,

Kildare, S., “Report on the Progress of Work on the Development of Finite Element Models of the FMVSS 214 and IIHS Side Impact Barriers”, GW Report, January 2005.

2 Human Facet Model Validation and Dummy Evaluation

2.1 Introduction

The objective of this task is to use either of the two MADYMO human models provided by TNO – finite-element and faceted – to create a model that accurately simulates occupant motion in far-side impacts. This model will then be used as the baseline for future modeling. An initial application included in this task will be the a comparison of the kinematics of dummy and human models in the far-side crash environment.

To date, anthropomorphic test devices (ATD's) have not been designed with consideration for human motion in far-side impacts. Thus leaving the question whether ATD's designed for frontal impacts or near-side crashes can adequately be used to model human motion in far-side. Previous tests with a BioSID dummy confirmed that the dummy does not suitably model the human motion, especially with consideration to the spine, since it is rather rigid. This was compared with a similar test with a human cadaver in far-side. (Fildes et al., ICROBI, 2002)

Previous MADYMO modeling by George Washington University National Crash Analysis Center showed that motion of a Hybrid III, BioSID, EuroSID 1, EuroSID2, or SID2s did not accurately reflect the motion of a human cadaver under the same impact configurations as a cadaver test of a far-side crash at Medical College of Wisconsin. (Alonso, 2004). These dummies mostly constructed with rigid spines did not exhibit the same excursion toward the far-side surface as the human cadaver did. Head contacts to the far-side surface are noted in real-world crash reconstructions under similar circumstances. Thus, we know that occupant displacement is farther than a current crash dummy predicts.

Figure 1 illustrates these MADYMO dummies compared with a cadaver test.

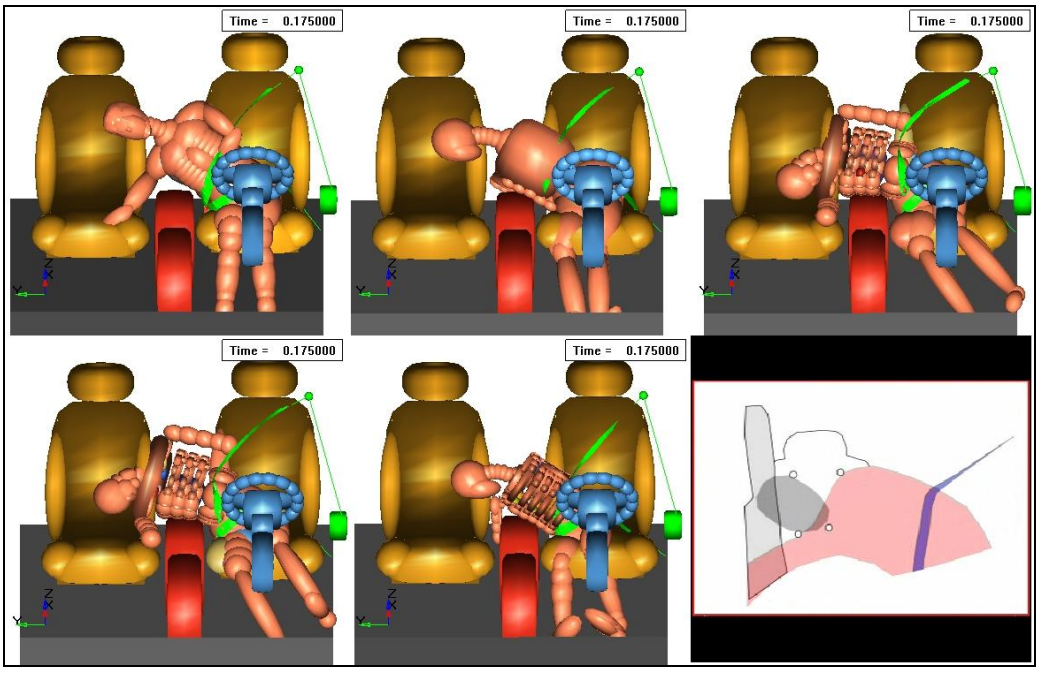

Figure 1: Dummy Models in Far-side with Cadaver Comparison - Hybrid III, BioSID, EuroSID 1, EuroSID2 and SID2s

From top left to top right, the dummies are Hybrid III, BioSID, and EuroSID 1. The bottom left and center are EuroSID 2 and SID2s, respectively. These dummy models were completed with a crash pulse from a 2000 Taurus side impact NCAP test at 62 kph. The cadaver video, at the bottom right, shows the head excursion of the dummy does not nearly match that of the cadaver in relation to the passenger seat. This cadaver test was performed at a slightly higher speed of 65 kph.

In addition to the ATD MADYMO models, TNO provides two human cadaver models. One based on finite elements and another more simple one with faceted surfaces. These two models are examined for suitability in far-side impacts.

2.2 Results

The TNO human finite element model proved to be difficult to use. First, the dummy cannot be initially positioned - the finite elements are fixed and validated in a certain position. Secondly, the runtime for the computer was extraordinary by MADYMO standards. It took a multi-processor machine 36 hours to run on 4 processors simultaneously. Finally, the model consistently went mathematically unstable. The meshed surfaces experienced extensive deformation causing the nodes to become chaotic and difficult to calculate further. The model could not run to completion. Figure 2 shows the human finite element simulation with theoretical center console pelvis support.

By examining figure 2, one must question the biofidelity of this model for far-side. The pelvis translation shown in the model is perhaps unrealistic. Also, the human model displayed extensive intrusion into the body, which a true human is unlikely to react in such a way with respect to the pelvis. It is noted that the model was developed and tested preliminarily for frontal impacts.

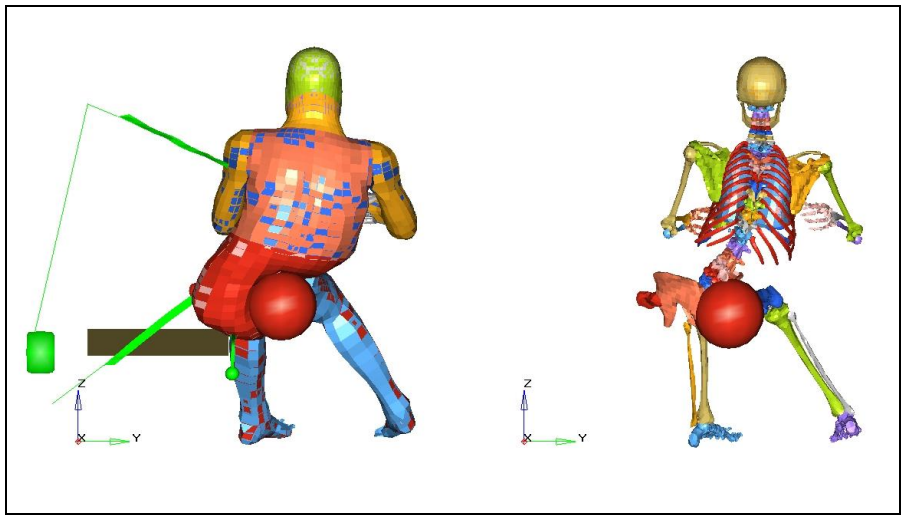

Figure 2: Human Finite Element Simulation

Conversely, the TNO human facet model showed promise when modeling a far-side crash. This model is simpler than the finite element model. It assumes rigid bodies surrounded by fixed nodes creating a faceted surface. Further, advantageous to this model is the representation of a flexible spine by modeling each vertebra with individual rigid bodies. Also, it provided flexibility in initial positioning by rotating joints for the knees, hips, shoulders, elbows, etc.

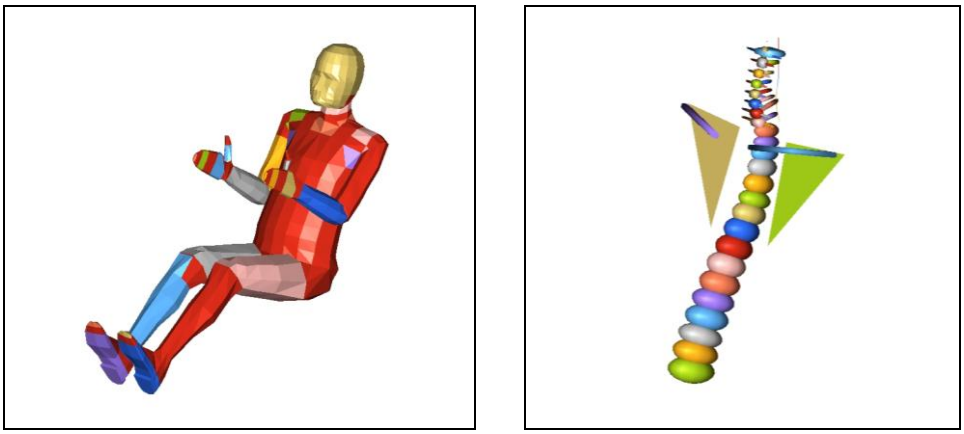

Figure 3: TNO Human Facet Model and Spine

Some modifications were made to the model in order to make the human properly react with the seat belts. It is difficult for MADYMO to mathematically calculate a facet to facet surface contact. The quantity and penetration of nodal surface into nodal surface is difficult to resolve. Therefore, additional ellipsoids were added to the human underneath the skin layer. These ellipsoids surrounded the same rigid bodies that the facets do, except are used for the belt contact surfaces instead of the facets. Ellipsoids were added for the rigid bodies making the pelvis, abdomen, shoulders, and upper arms. Besides the seat belt contacts, these ellipsoids are inconsequential to the rest of the model.

Upon placing the human facet model into the interior of the vehicle, positioning it properly, and defining the contact functions; the model duplicated the motion of the cadaver quite well. The excursion and upper body motion of the two were similar. Figure 4 shows the two synchronized at discrete time steps.

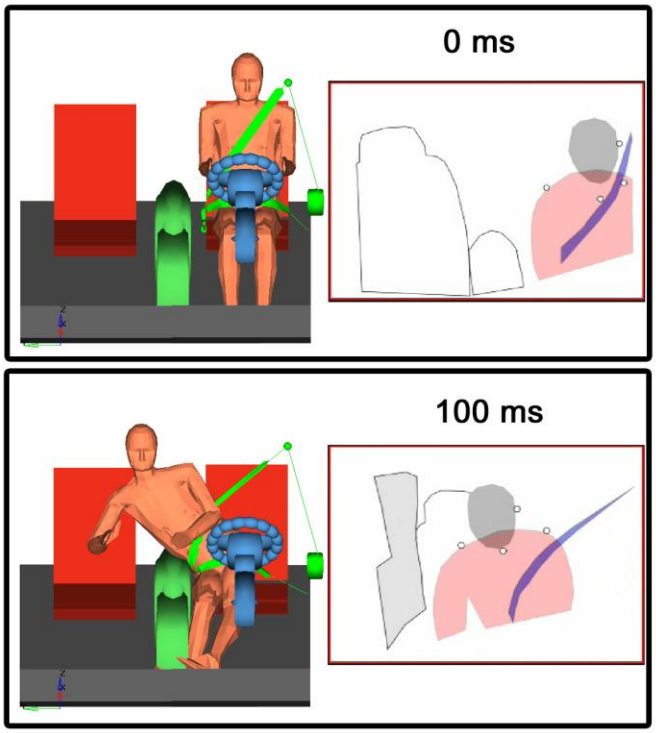

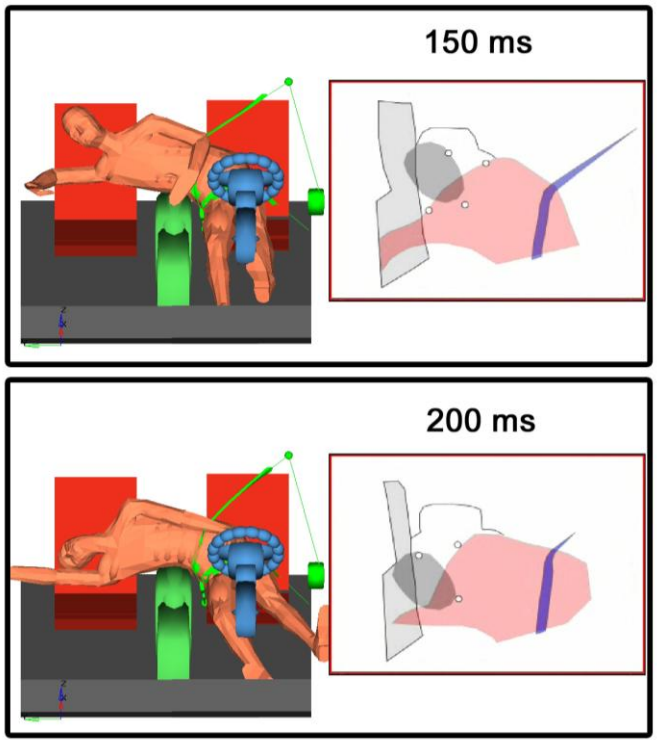

Figure 4: Human Facet Model with Cadaver Comparison

The crash pulse recorded during the cadaver test was used as the input for the MADYMO model. This pulse measured the lateral acceleration of the Holden Commodore as it was struck on the far-side. Figure 5 below shows this acceleration plot.

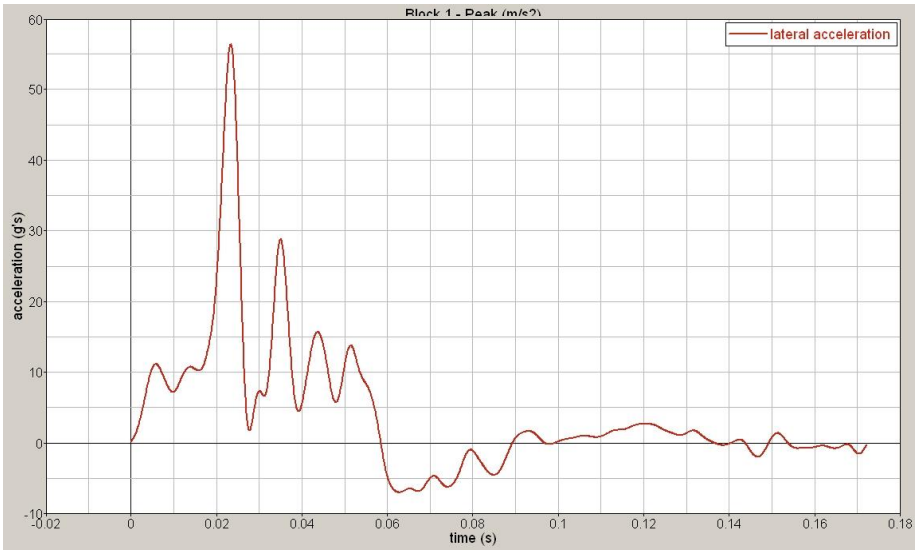

Figure 5: Far-side Cadaver in Holden Commodore Pulse

One difference between the two models is noted in the shoulder belt. In the MADYMO model, the shoulder belt easily falls off the occupant. In the cadaver, some light friction keeps the belt on the occupant. In the MADYMO model, it is difficult to model friction between to faceted surfaces, which may explain this.

To further examine the human facet model, a direct comparison with a Hybrid III MADYMO model was made. A pulse from an IIHS barrier test was used to excite both models simultaneously. Figure 6 below shows snap shots of the two at 0, 100, and 150 milliseconds.

The vertical line through the passenger seat estimates the maximum intrusion distance from the impact. This estimation comes from a finite element vehicle model conducted at the GWU – National Crash Analysis Center (Digges et al, AAAM, 2005). The difference between the human facet model and Hybrid III is clear when examining the occupant excursion towards the impact. The head of the human facet model traveled approximately 30cm further than the Hybrid III.

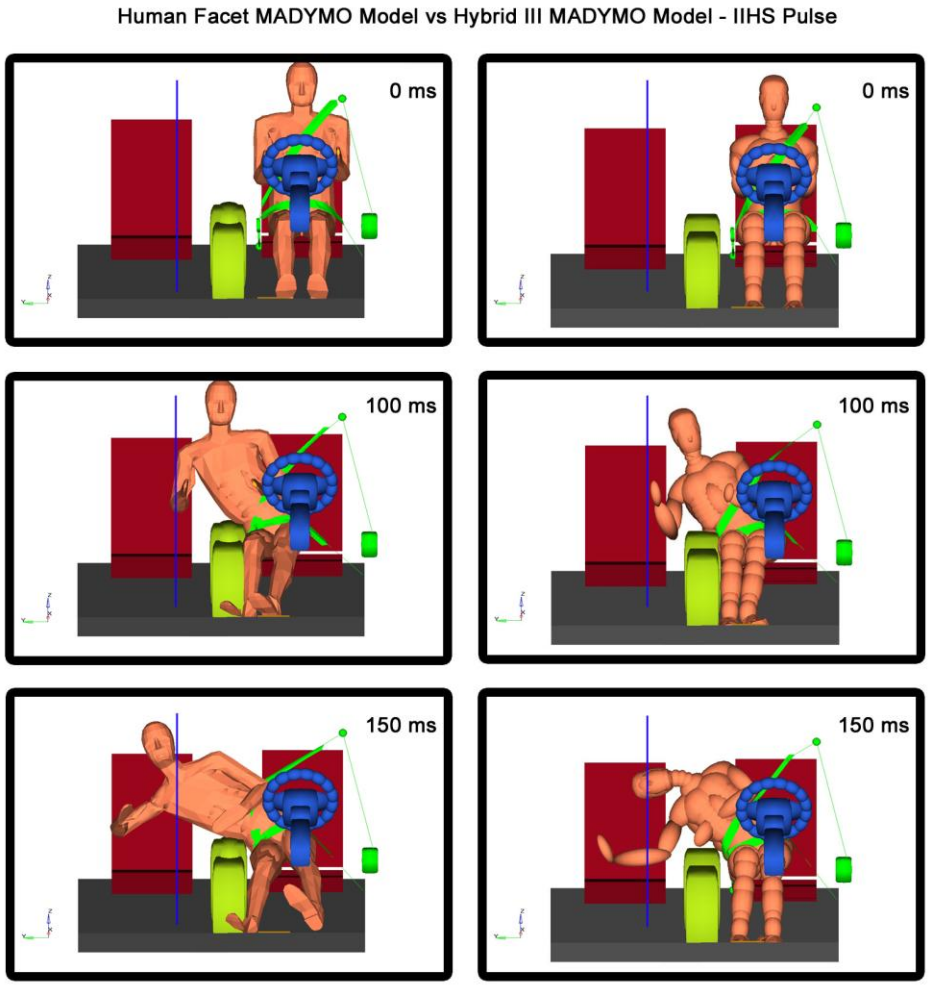

Figure 6: Human Facet MADYMO Model vs. Hybrid III MADYMO Model

2.3 Conclusions

Using visual approximations, the human facet model moved similarly to a human cadaver test under the same impact configuration. Using this single test as a benchmark, comfort was gained in this model – it moved more similar to the human than any crash dummy or other computer model did. In contrast the human finite element MADYMO model seemed not to be too realistic, and it was difficult to use.

As shown in Figures 1 and 6, the MADYMO dummy models (Hybrid III, BioSID, EuroSID 1, EuroSID2, or SID2s) did not accurately reflect the motion of a human cadaver under the same impact configurations as a cadaver test.

In the future, this model should be refined and correlated to more cadaver tests. Parameters such as chest and head acceleration plots should be examined more closely and checked for correctness.

2.4 References

Alonso, B., *Far-side Impact Simulations with MADYMO,* Report written to George Washington University – National Crash Analysis Center, October 2004.

Digges, K., Gabler, H., Mohan, P., Alonso, B. *Characteristics of the Injury Environment in Far-side Crashes*. Association for the Advancement of Automotive Medicine, 2005.

Fildes, B., Sparke L., Bostrom O., Pintar, F., Yoganandan N., and Morris, A. *Suitability of Current Side Impact Test Dummies in Far-side Impacts*, Proceedings of the 2002 International IRCOBI Conference on the Biomechanics of Impact, Munich, Germany, September 2002.

3 Effect of Center Console Height on Dummy Kinematics

3.1 Introduction

The objective of this task is to use the MADYMO computer simulation tool to examine the effects of center console height on occupant motion in far-side impacts.

When examining occupant motion in far-side impacts, it is apparent that few countermeasures exist to limit motion towards the far-side surface. Occupant head strikes to the far-side surface (a-pillar, door, roof, or b-pillar) are observed in real world crash investigations. This is also confirmed in cadaver testing with full vehicle to vehicle collisions.

For belted occupants, which this study limits itself to, the lap portion of a 3-point seatbelt helps to keep the occupant's pelvis in the seat. However, the shoulder belt provides little resistance for the upper body, while the lap portion keeps the pelvis in place.

The center console also prevents the pelvis and abdomen from translating towards the impact. However, the size, shape, and even presence of a console vary among vehicle models.

This study uses MADYMO computer simulations with the human facet-model to study changes in height of the center console with belted occupant motion.

3.2 Methods

A previous Task with MADYMO modeling, reported in Section 2, found the TNO human facet model placed inside a simplified vehicle model visually correlated rather well to a similar cadaver test. This grossly validated model served as the foundation for the center console experiment. The model contained on occupant seated in the normal driving position with a steering wheel, center console, transmission tunnel, and a 3 point belt system.

The lateral acceleration pulse from the cadaver test performed by Fildes et al. with a Holden Commordore was used as the input for each run (Fildes et al IRCOBI 2002). Only the y-direction acceleration was considered, ignoring x, z, roll, pitch, and yaw accelerations. Figure 1 plots the acceleration.

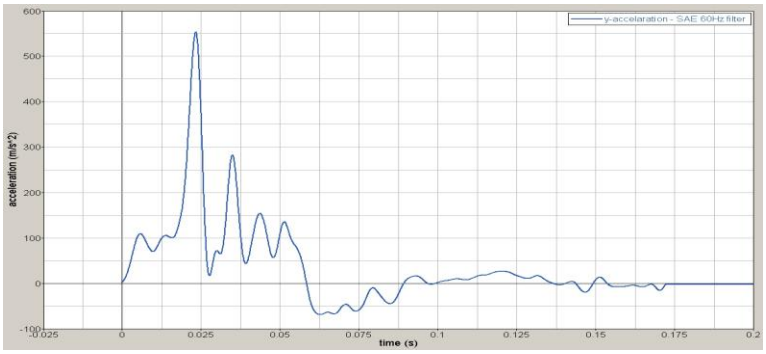

Figure 1: Lateral Acceleration Pulse

10 different levels for the center console were chosen. First, the center console was made flush with the driver and passenger seats. Each iteration of the model raised the center console by 25 mm (approximately 1 inch). The center console started out as flush then moved up by one inch until standing 10 inches above the seats.

3.3 Results

Upon using the pulse in Figure 1 in the human facet model, the following snapshots show the model with 6 different center console height measurements.

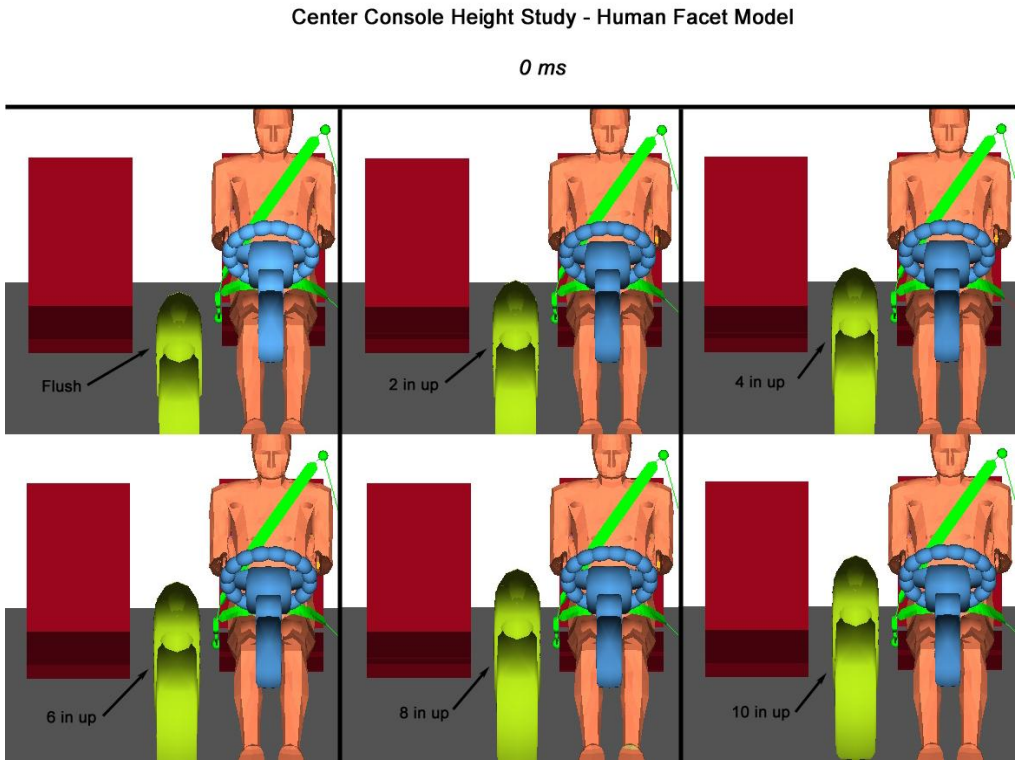

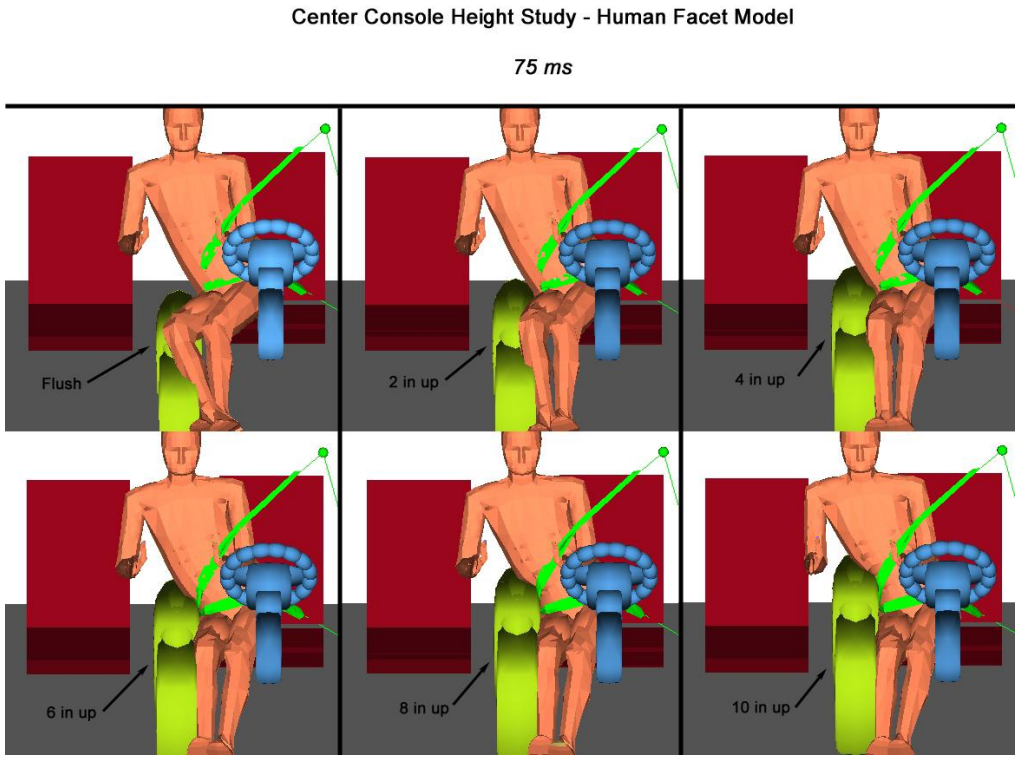

Center Console Height Study - Human Facet Model

100 ms

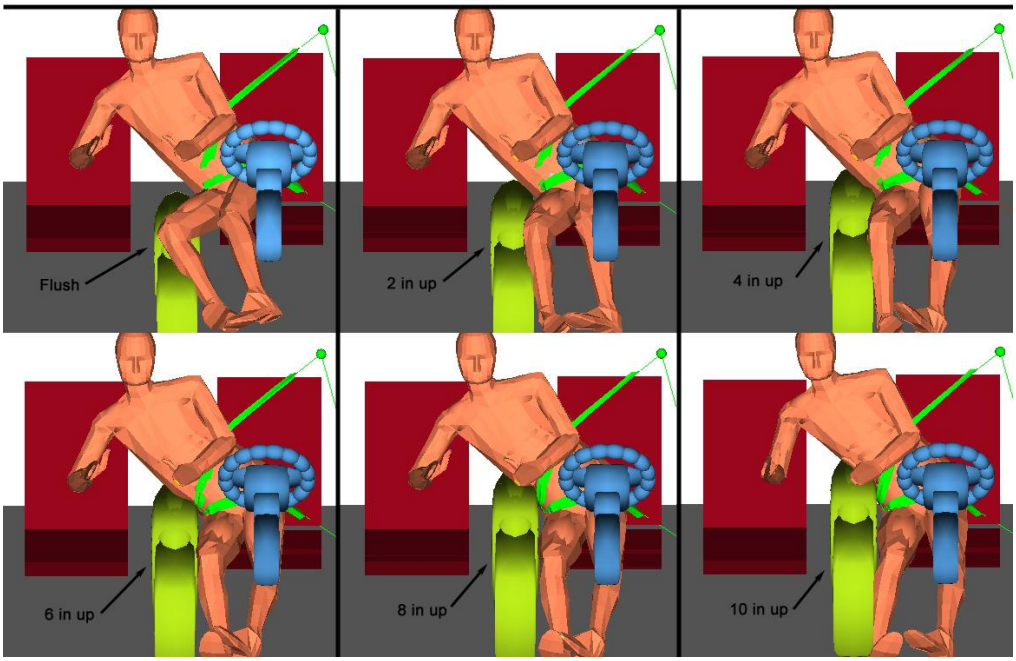

Center Console Height Study - Human Facet Model

125 ms

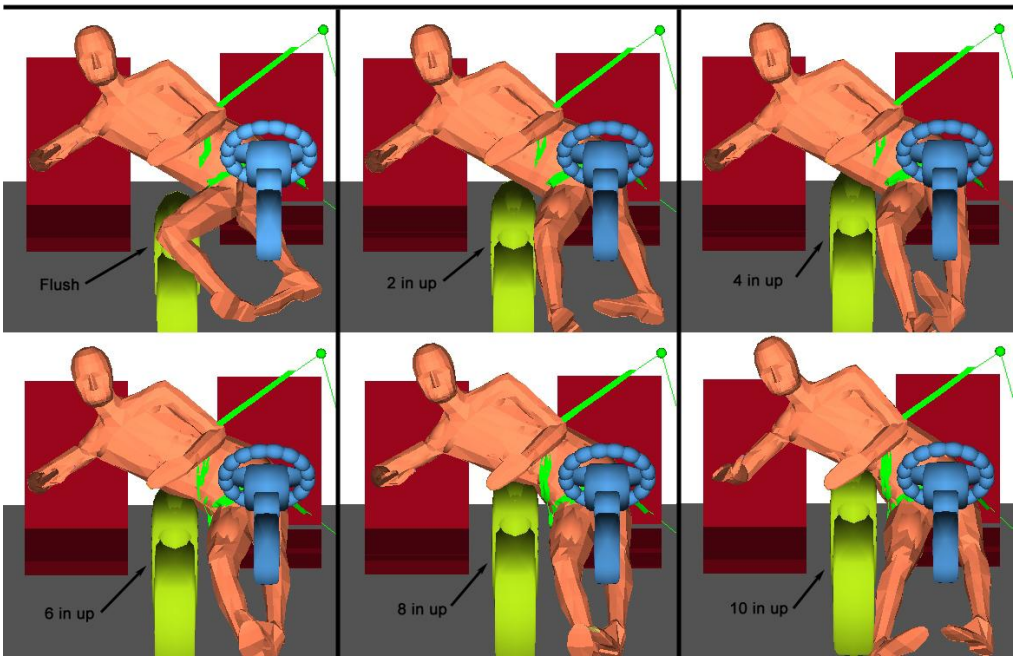

Center Console Height Study - Human Facet Model

150 ms

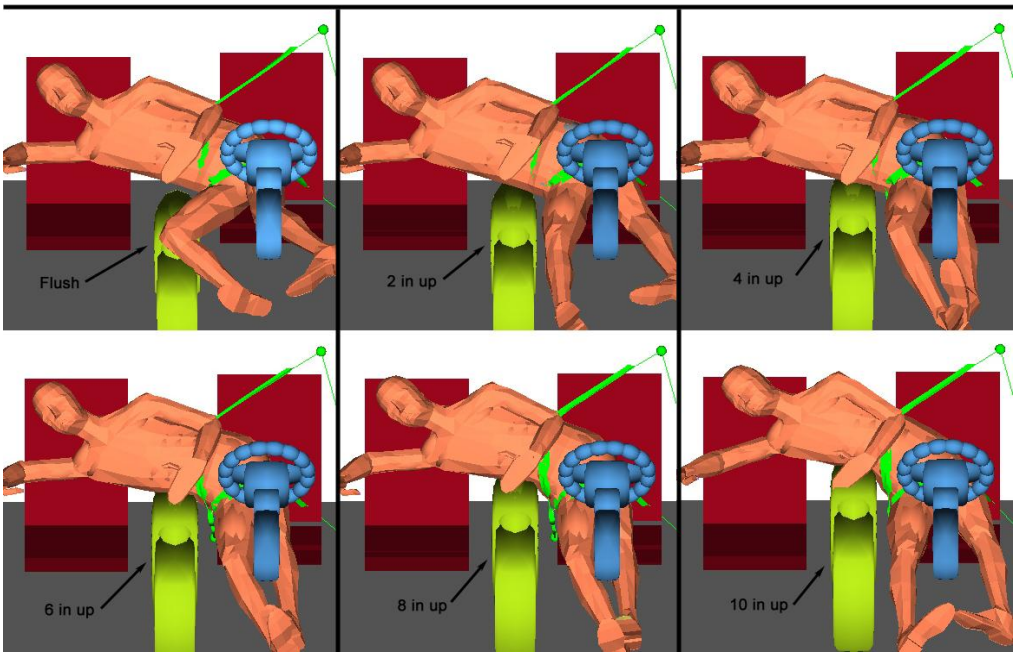

Center Console Height Study - Human Facet Model

175 ms

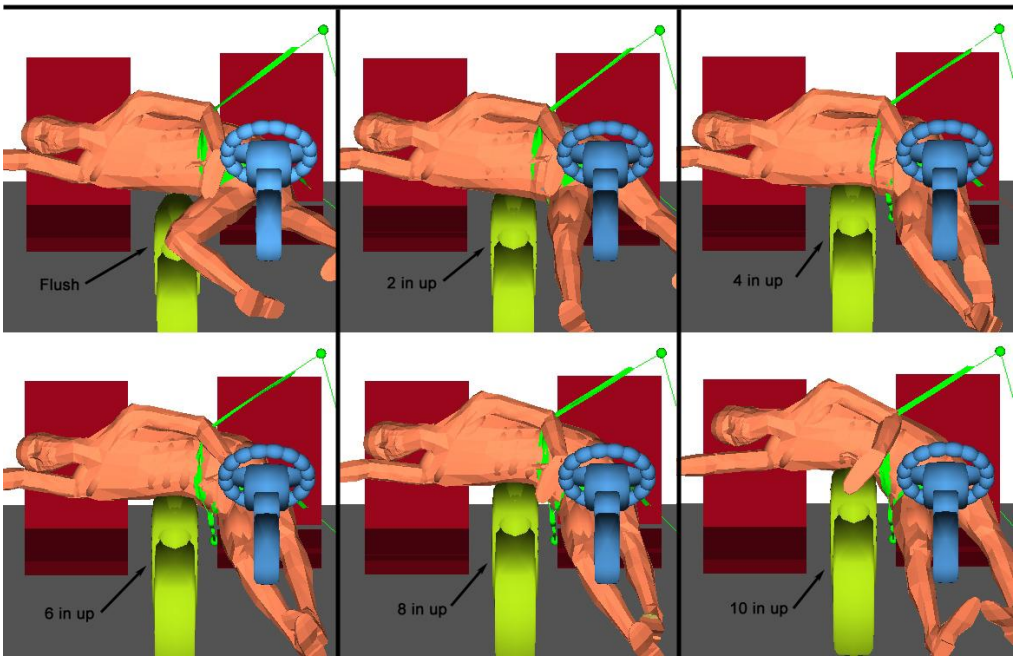

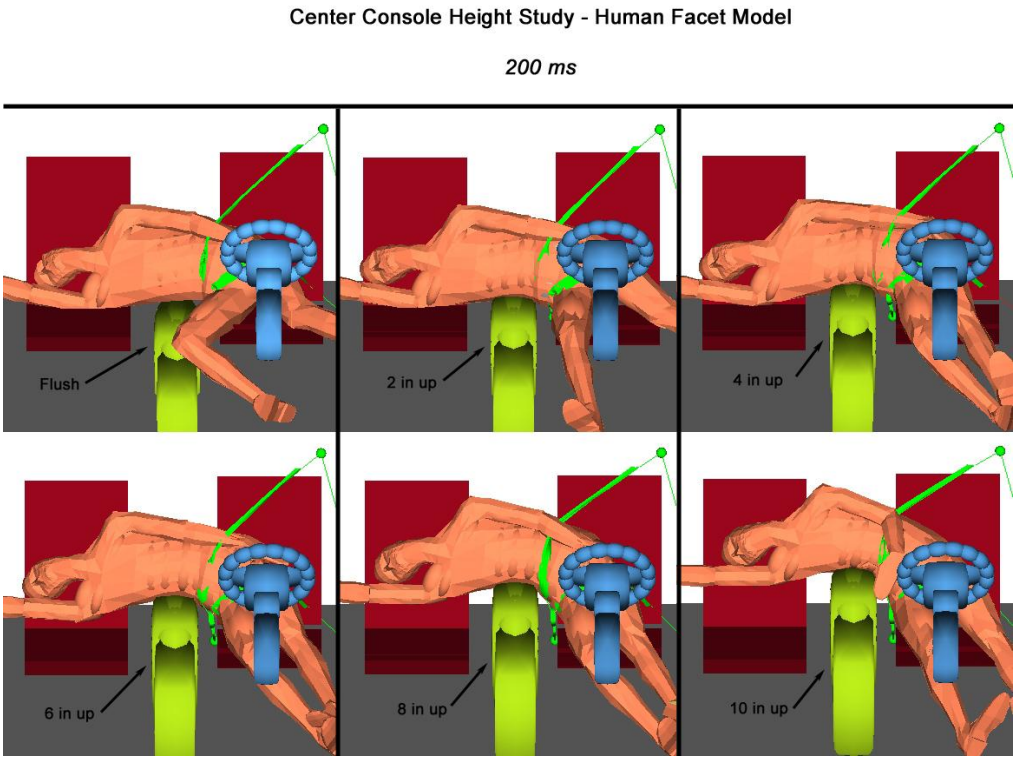

Figure 1. Snapshots of human kinematics - six different console heights and seven time increments

Furthermore, MADYMO calculated the combined forces placed on the center console for each iteration. Figure 2 shows the peak force for each center console height.

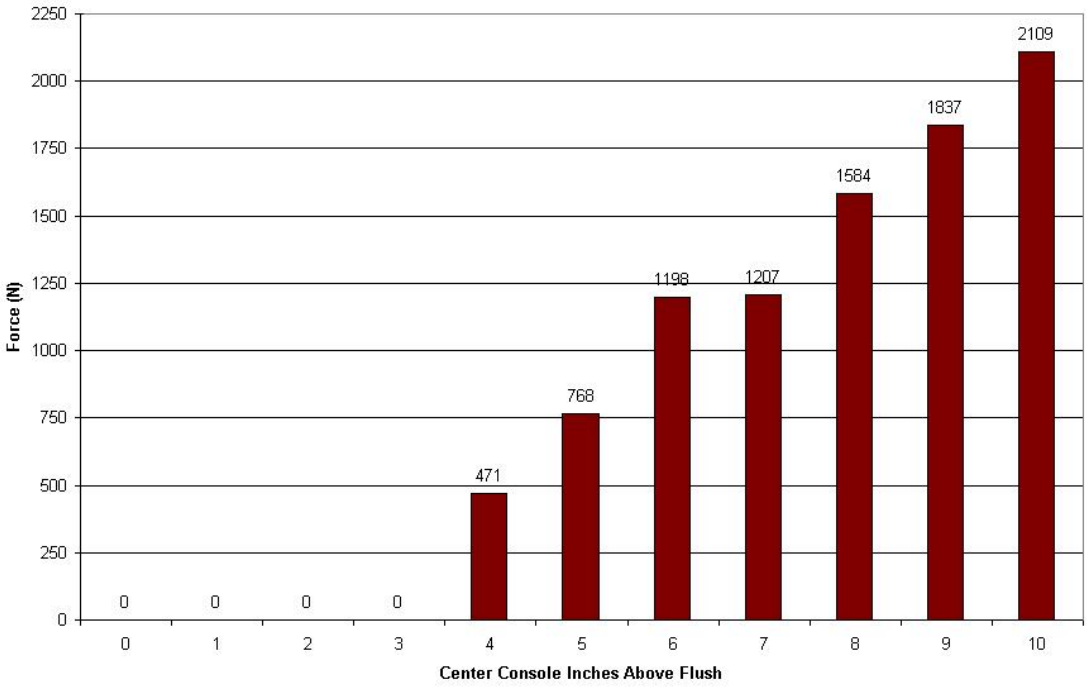

Figure 2: Center Console to Occupant Peak Force

Figure 3 shows the lap belt forces used by MADYMO at 2 inch intervals.

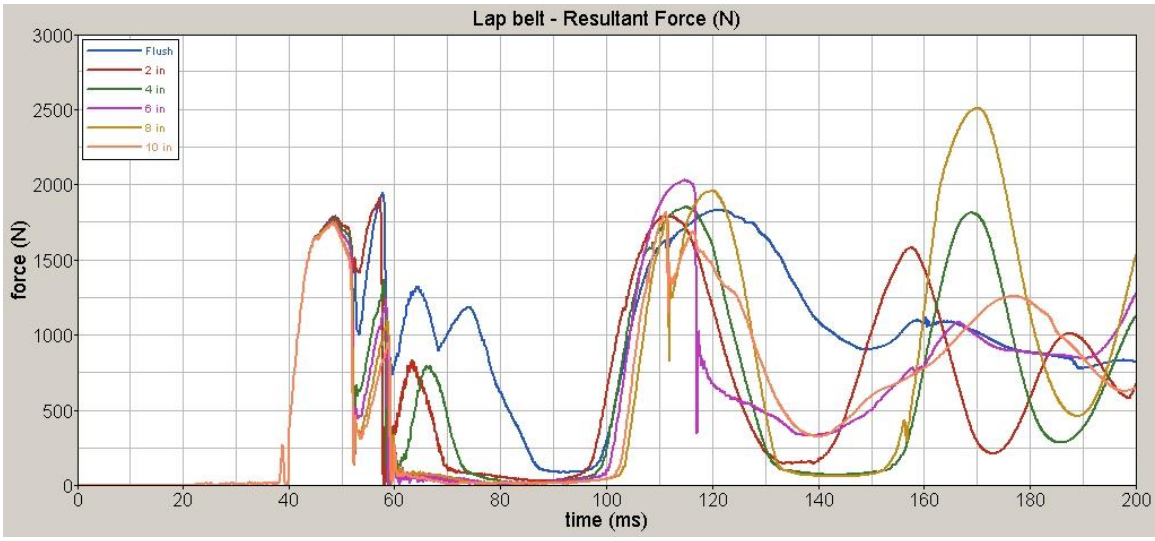

Figure 3: Lap belt forces

3.4 Conclusions

The model predicts that the height of the center console changed the occupant excursion slightly, perhaps not as much as would be expected. The force exerted by the occupant on the center console increased as the height of the center console increased, however, when the center console remained low, the belt restraint system restrained the pelvis rather than the center console.

It appears that as the center console height increased above 8 inches, it loaded the occupant's abdomen and ribs. However, this was not measured on the MADYMO model due to the difficulty of using the faceted surfaces.

The plots for the lap belt force numbers are inconclusive at this point. The human facet model used has not been correlated to a test and the forces have not been checked for correctness. From the plot in figure 3 it is seen that the magnitudes of the belt forces did not change significantly as the center console height changed, especially within the first 60 milliseconds. This could be interpreted that the lap belt holds the restrains the pelvis regardless of center console height. Beyond this the shape of the plots move rather erratically. This is when the pelvis moves upward over the center console, which changes as the center console changes.

3.5 References

Alonso, B., *Far-side Impact Simulations with MADYMO,* Report written to George Washington University – National Crash Analysis Center, October 2004.

Alonso, B., MAYDMO Human Facet Model Validation for Far-side, Memo written to George Washington University – National Crash Analysis Center, October 2004.

Fildes, B., Sparke L., Bostrom O., Pintar, F., Yoganandan N., and Morris, A. *Suitability of Current Side Impact Test Dummies in Far-side Impacts*, Proceedings of the 2002 International IRCOBI Conference on the Biomechanics of Impact, Munich, Germany, September 2002.

4 Suitability of Square Acceleration Profile for Far-Side Impact Testing

4.1 Introduction

The objective of this Task is to use the MADYMO computer simulation tool to determine whether a square acceleration pulse of equal energy to a peaked crash pulse is suitable for far-side cadaver Hyge sled tests.

The Hyge sled at Medical College of Wisconsin was designed to run square shaped deceleration profiles. This sled will be used for future far-side human cadaver or dummy experiments.

A previous cadaver test for far-side utilized a full-vehicle - Holden Commodore. This vehicle was struck on the far-side according to ECE 95 protocol. The test produced a multi-peaked acceleration pulse, as measured in full-vehicle crashes (Fildes et al., ICROBI, 2002).

Figure 1 contains an overlay of the full-vehicle pulse and a square pulse from the test buck at MCW. Both deceleration curves contain equal energy.

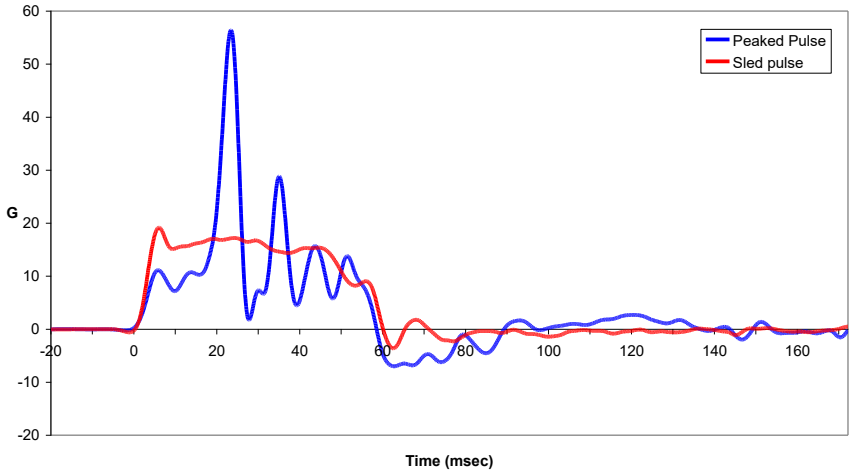

Figure 1: Peaked and Square Lateral Acceleration

4.2 Results

The two curves from Figure 1 were used as the input for a MADYMO model with the TNO human faceted occupant. The model was only accelerated in the y-direction (lateral) according to the curves. Any accelerations in the x or z directions were ignored, in addition to not accounting for vehicle roll, pitch, and yaw. Both simulations were run from 0 to 200 milliseconds. For any time beyond 170ms, the acceleration was assumed to be 0 $^{m}/_{s^2}$.

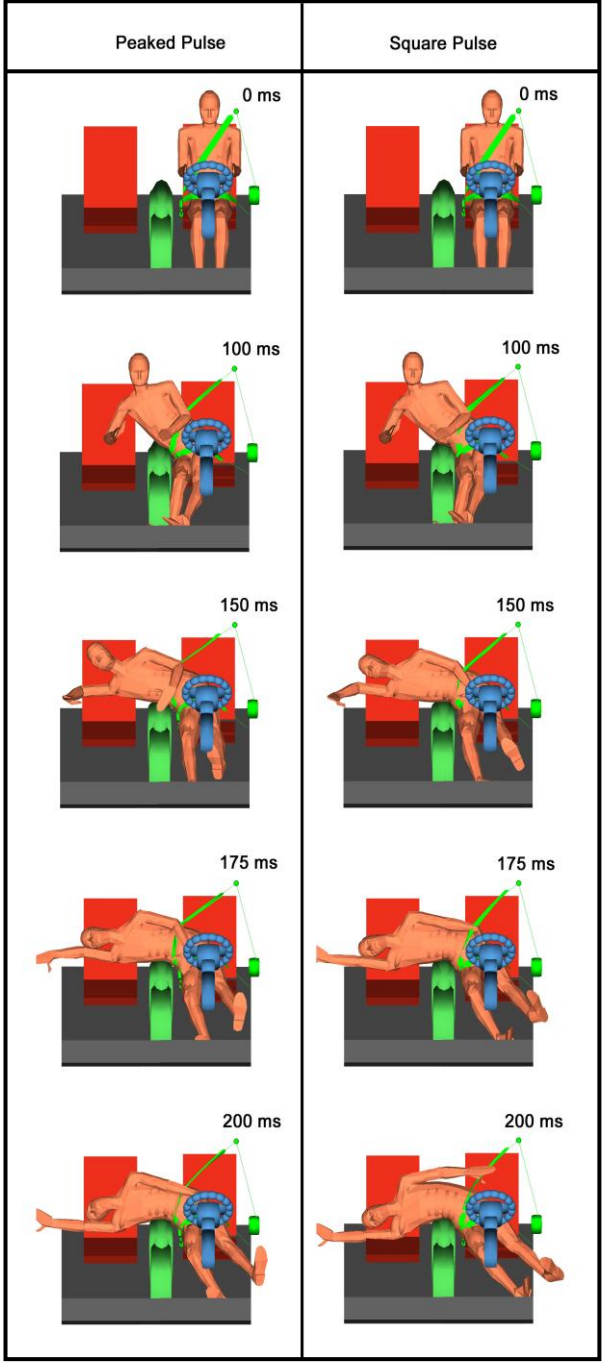

Figure 2: Human Facet Model with Peaked and Square Pulses

Figure 2 contains snapshots of the two animations simultaneously.

The model predicted the occupant excursion in a square wave impact was slightly greater than the excursion in a peaked wave impact, this is demonstrated in the snapshot at 175ms. Also, the occupant's reaction to the peaked pulse is delayed to that of the square pulse. This is evident at the snapshot taken at 150ms.

The Figures 3, 4 and 5 below are the pelvis, chest, and head acceleration time histories for the human facet model when subjected to the two different pulses.

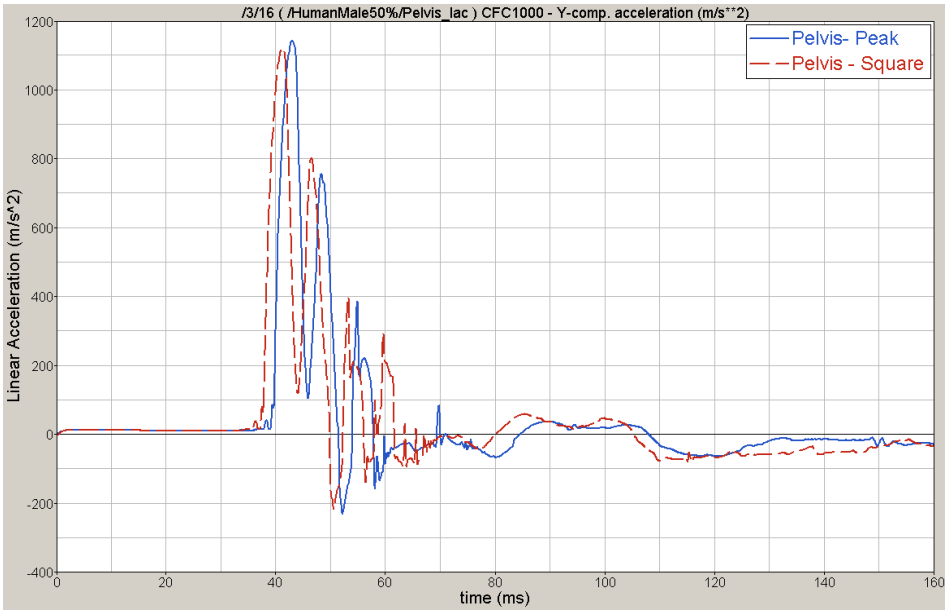

Figure 3. Pelvic Acceleration

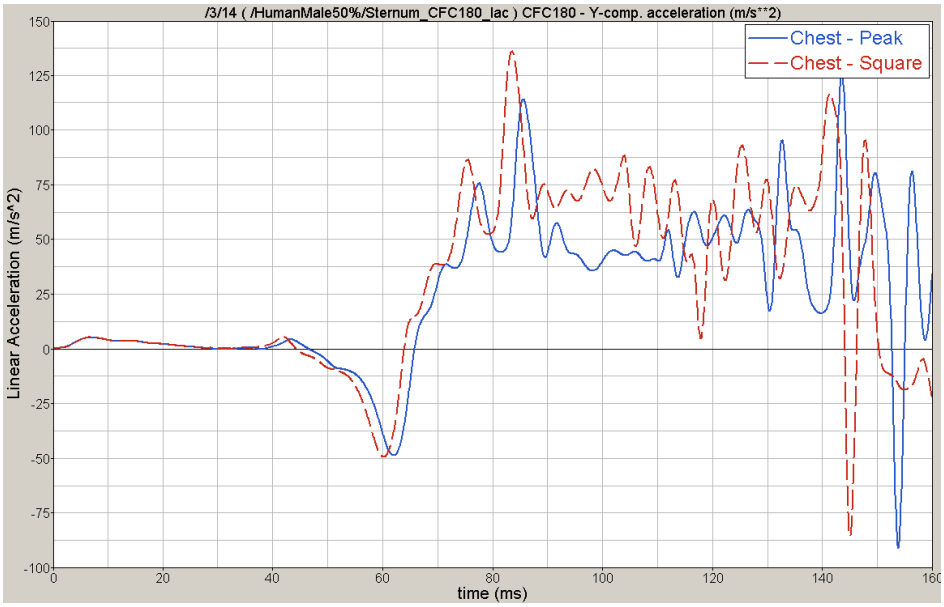

Figure 4. Chest Acceleration

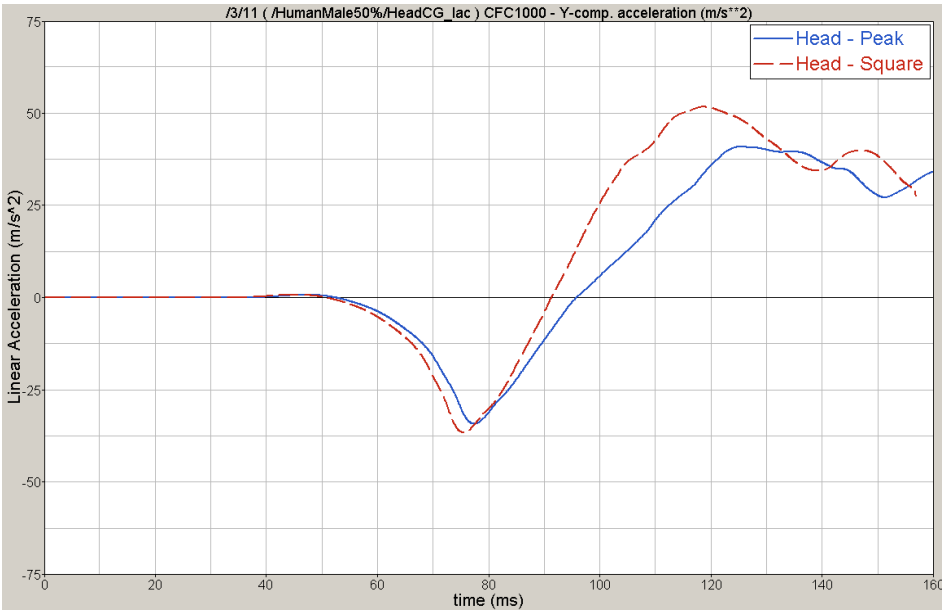

Figure 5. Head Acceleration

4.3 Discussion

When visually examining the two human facet models together, minor differences are noticeable. The human model subjected to the square acceleration plot had slightly higher excursion toward the impact, approximately 4 cm further. In addition, the human model subjected to the square pulse traveled forward in time when compared to the peaked pulse by 5 to 10 ms. However, the path of motion between the two remained quite similar.

When analyzing the pelvis, chest, and head acceleration recorded by MADYMO, the two simulations demonstrated similar magnitudes and shapes, however, the occupant reactions during the square wave simulation were shifted earlier in time by a few milliseconds. These kinematics may be explained because the square acceleration profile slopes up more quickly and continues to accelerate the occupant, while the peaked pulse drops lower before peaking again. The constant acceleration from the square wave gets the occupant moving more quickly to the center console.

4.4 Conclusions

Despite these differences in excursion distance and time delay - which ought to be noted – the motion of the two human remain remarkably similar based on these results from MADYMO modeling. Nearly the same result was achieved between the two with acceleration pulses of equal energy. Similar peak acceleration magnitudes of the head, chest, and pelvis were produced.

4.5 References

Alonso, B., *Far-side Impact Simulations with MADYMO,* Report written to George Washington University – National Crash Analysis Center, October 2004.

Alonso, B., MAYDMO Human Facet Model Validation for Far-side, Memo written to George Washington University – National Crash Analysis Center, October 2004.

Fildes, B., Sparke L., Bostrom O., Pintar, F., Yoganandan N., and Morris, A. *Suitability of Current Side Impact Test Dummies in Far-side Impacts*, Proceedings of the 2002 International IRCOBI Conference on the Biomechanics of Impact, Munich, Germany, September 2002.

5 Far-Side Impact Vehicle Simulations with MADYMO

5.1 Introduction

Collisions occurring on the far-side of the vehicle to the occupant position account for a significant portion of automotive fatalities and HARM annually. All side impacts generally account for 35% of road trauma (Fildes 2002). Of these side-impact injuries, those resulting from impacts on the far-side of the vehicle account for 40% of HARM (Fildes, Digges, etc.). Despite these statistics, most research and regulations to date for side-impacts are dedicated to near-side, without further understanding of injury mechanisms of far-side.

Impacts on the far-side are most commonly characterized by a head injury and fewer chest and abdominal injuries (Fildes 1994). These outcomes stem from occupants excursion out of the seat and contacting the far-side door, impacting vehicle or object, or occupant (Fildes 1994). This same excursion and occupant kinematics are not seen in near-side impacts due to the nature of the event.

Since most side impact research and regulations are focused on near-side impacts, side-impact dummies are designed to consider injury criteria and biofidelic requirements of near-side hits. These are characterized by broad intruding impacts to one side of the body. Conversely, far-side is marked by excursion out of the seat and towards source of impact. Typical modern vehicle interior arrangements are limited in the ability to hold the occupant in place during this situation and thus results in upper torso movement and spinal bending. Meanwhile, the occupant usually absorbs near-side impacts in the ribs and hips. The stark differences in these two side-impact scenarios places the suitability of current side-impact ATDs for far-side impact testing into question.

Fildes, Sparke, Bostrom, Pintar, Yoganandan, and Morris reported that current WorldSID prototype and BioSID dummy with a modified lumbar spine provide the most reasonable simulations to occupant kinematics and injuries. This study was based upon comparison of a Post Mortem Human Subject (PMHS) and four ATDs – BioSID, BioSID with lumbar spine modification, EuroSID 1, and WorldSID. Some of the metrics used to evaluate these dummies to the PMHS were torso shear, spine straightening, and head impact. The authors reported that the BioSID, EuroSID 1, and WorldSID did not reproduce a head strike with the far-side door as the PMHS did.

This paper seeks to further evaluate these dummies and others by using computer simulations to assess dummy responses in far-side impact scenarios and measure their responses to countermeasures. For thoroughness, multiple angles and multiples speeds were used in the simulations.

5.2 Methodology

The model work commenced with a previous MADYMO model designed primarily for frontal impacts. It contained a Hybrid III crash test dummy seated inside a full vehicle interior. From this, any vehicle acceleration could be applied linearly in the x, y, or z-axis directions, concurrently with rotational accelerations around the three axes. Contact interactions and force deflection functions between the dummy and vehicle interior were previously defined in the model. The first far-side simulations began by applying y-axis acceleration pulses for a side impact test to this same model.

Upon deleting the Hybrid III dummy from the model, the remaining vehicle interior was used as the basis of future simulations with other dummy models. The original model was written in MADYMO Version 5.4 and converted to MADYMO 6.0.1 in XML computer language. All further modeling conducted in MADYMO 6.0.1 table format.

5.2.1 Vehicle Interiors

The vehicle interior, loosely based on 1999 Ford Taurus geometry, used mostly ellipsoids to represent interior surfaces. These ellipsoids connected to each other through rigid joints. Computationally, ellipsoids are the easiest for MADYMO to process, as opposed to faceted surfaces, for increased model performance. Planes were used in some locations such as floorboard, dashboard, and roof. Although the seat appears to be constructed of ellipsoids, actually a plane existed underneath the ellipsoids for seat bottom and another for seat back contact interactions, instead of making contact with the seat ellipsoids. The vehicle configuration is pictured in figure 1.

This interior model contained a number of supplemental safety devices found in modern vehicles. A 3-point belt restraint system surrounded the driver. This belt had the option of having belt force limiter and pyrotechnic pretensioner, both of which could be turned on or off inside the input file code. An airbag could also be placed in the steering column of the model, however, the airbag does not deploy in side-impacts, and not used in these simulations.

The interior was broken into two portions - the passenger-side and driver-side. The driver-side included driver seat, instrument panel, and steering column. The passenger-side contained the passenger seat, center console, and armrest. The seatbelt system moved during the impact and was thus not a part of either driver-side or passenger-side rigid systems. It was instead included in the inertial space.

To better organize the code of the original model, each ellipsoid and plane of the interior had a characteristic function associated to it, an advantage of MAYDMO Version 6. These functions were pulled from a library of function in the original Hybrid III model. The mathematical purpose of these functions was for when another ellipsoid penetrated this interior representing ellipsoid, the function would determine the amount of force to exert back by measuring the distance penetrated. This function was combined with the characteristic function of the penetrating ellipsoid to determine a final force-deflection function.

TNO, the suppliers of MADYMO code, provide several computer models of crash test dummies. Of the many supplied, the one's chosen for this study were – BioSID, EuroSID I, EuroSID II, SID2s, and human finite element model. Also, of interest would be the WorldSID model, however it does not exist. All side-impact dummies (SID's) used were right-hand impact oriented.

5.2.2 Dummies and Initial Setup

After inserting each new dummy into the vehicle interior, two processes needed to be followed to properly setup the model – dummy rest positioning and initial belt positioning.

After inserting the dummy into the model and properly defining all environmental contact functions, rough dummy positioning was visually achieved through EASi-Crash software. To further specify the correct dummy position, gravity ($-9.81 m/s^2$ linear acceleration in z-axis) was applied to each rigid body of the particular dummies. No other accelerations or inputs were specified. The model was run for a long duration of time, allowing the dummy to fall to resting position and reach equilibrium with the interior. The final joint positions at equilibrium were taken from the appropriate output file and placed in the model.

To position the belts, each end of the lap or shoulder belt was gently accelerated towards its anchor. The dummy was locked in place and made rigid during this process. The process gently contoured the belt around the respective dummy. For each cycle, the belt nodal positions at the desired point in time were copied into the program and used as the initial positions for the next simulation.

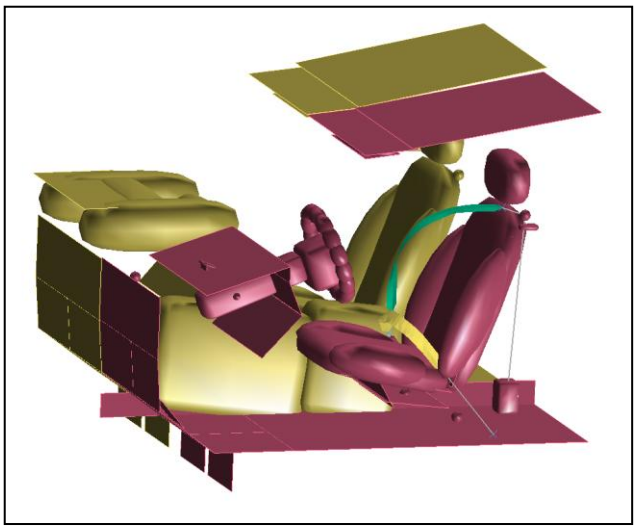

Figure 1: Vehicle Interior

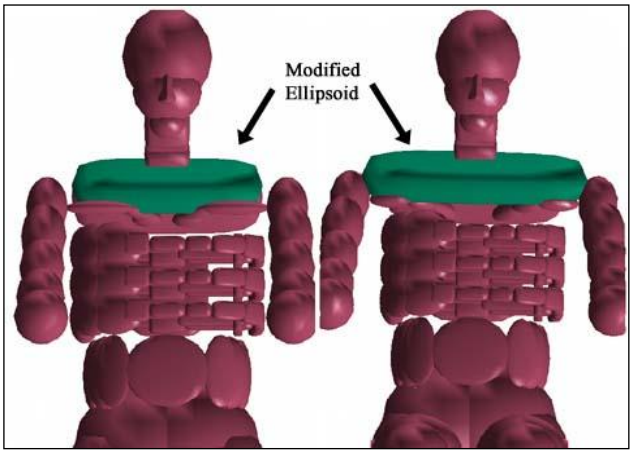

Figure 2: EuroSID Shoulder modifications

5.2.2.1 BioSID

The BioSID crash dummy, based upon a 50th percentile adult male, contains legs, head, and neck similar to Hybrid III. The BioSID rigid spine supports 6 deformable ribs for near-side impacts. The ribs mount on the left-side for left impacts and right-side for right impacts. This particular model used a right-side dummy to study far-side impacts to the driver.

The BioSID MADYMO model, developed at the time of the old Hybrid III non-segmented neck, needed updating with the current more biofidelic segmented neck. The updated neck is modeled and contained in the Hybrid III MADYMO model, however, not found in the BioSID MADYMO model. For purposes of far-side simulations, dummy neck responses were important to study, therefore necessary to update. The released BioSID MADYMO model was designed and validated against a dummy with the old non-segmented neck.

Updating the BioSID with the new neck created a non-validated model, however, assumed to be suitable. The new used the exact same underlying code and properties for the Hybrid III segmented neck. This was copied and inserted to the BioSID model between the same two rigid bodies as the old neck, as seen below. The heads are identical in BioSID and Hybrid III and both use a rigid plate between the shoulders for a base.

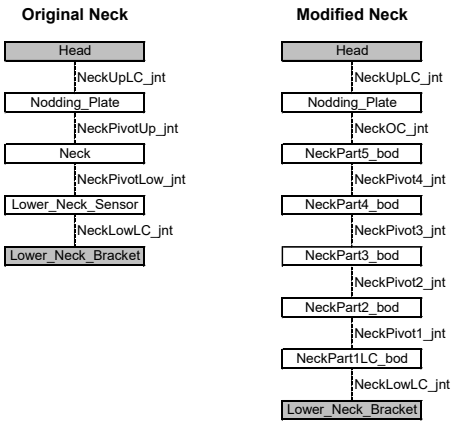

As shown, the new neck added extra bodies and joints between the head and shoulder, but maintained the same distance between start and end points.

5.2.2.2 EuroSID I & II

The EuroSID I and II MADYMO models appear identically, however, differences exist in a couple joint properties and configuration, particularly in the shoulders and chest areas.

Due to this unique application of EuroSID models for far-side instead of near-side for which it was designed, a challenge arose with the seatbelt interactions. Typically for near-side impacts, the shoulder seatbelt gets trapped in the shoulder neck region while the dummy contacts the door. For far-side, the upper torso of the human/dummy moves laterally toward the passenger seat, sliding the shoulder belt off the outside shoulder. In the EuroSID models, a valley exists between the collar bone ellipsoid and shoulder ellipsoid. The seatbelt dropped into this valley on initial simulations and unnaturally restrained the driver.

To correct the grabbing problem, the collar bone ellipsoid was extended laterally for both the EuroSID I and II models to overlap the shoulder ellipsoid and allow the shoulder belt to slide of the shoulder during occupant excursion to the far-side. Figure 2 shows the original ellipsoid configuration and the modified EuroSID.

5.2.2.3 SID2s

The SID2s, based on 12 to 14 year-old adolescents, was the only petite sized occupant model evaluated for far-side impacts. The same procedure was followed as with the other models – gravity used to pull the model into position and seatbelts pulled snug over the pelvis and chest.

The resulting initial simulations displayed some challenges with the seatbelt and torso interactions. The model, again designed for near-side impacts, contains 6 thin ribs for the upper body. When the shoulder belt moved to restrain the ribs, the nodes of the belts fell between the ellipsoids and the shoulder belt acted transparent to the chest. To alleviate the situation, the faceted mesh for the shoulder belt was made twice as fine, thereby created more nodes closer together and more contact points for the belt to ellipsoid.

5.2.2.4 Human Finite Element Model

The human finite element model released by TNO Automotive is the most detailed and sophisticated of any of the preceding models. Based upon cadaver data, the model uses faceted bone models and layers of finite elements for deformable tissue. The model contains true skeletal and organ geometry. It visually appears as a human rather than dummy.

The model begins with the cadaver in a seated position with arms extended forward. Unfortunately, the model is limited against positioning the human out of this initial setup. Therefore, gravity was not used to position the dummy.

Due to the complexity to the model, run time was an important consideration. To simplify the model, all environmental surfaces were removed, except the planes for the seat and ellipsoid for center console.

The model was computed using 4 processors simultaneously to improve run-time.

5.2.2.5 Human Faceted Model

A more simplified cadaver experimental model is also released by TNO. This uses rigid bodies and faceted surfaces. Using the pre-defined contact groups, the dummy was placed in the vehicle interior, and positioned. The belts were contoured around. Due to difficulties with two faceted surfaces contacting one another, as with the belts to the faceted human model, ellipsoids were placed underneath the skin facets to improve the belt contact properties.

5.2.3 Crash Pulses

For these far-side simulations, the acceleration pulse was taken from a US New Car Assessment Program (NCAP) NHTSA 214 test of a 2000 Ford Taurus SE 4-door. The x and y plots are displayed below in figure 3 (the plot of large amplitude is y-axis acceleration). The vehicle was struck on the near-side, and the y-component multiplied by -1 to make it far-side for simulations. This case was almost a true 90 degree impact, only a small acceleration is seen for the x-axis.

Additionally to understand far-side impacts, the pulse was rotated 45 degrees towards the front and repeated for all simulations. The rotation was accomplished by multiplying the appropriate functions by cosine and sine of 45 degrees and adding together.

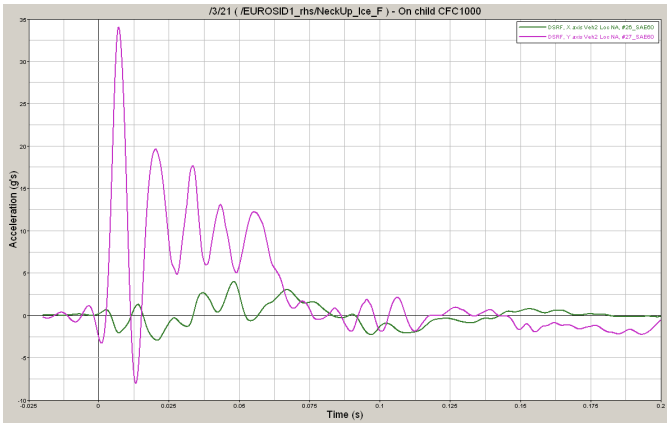

Figure 3: NCAP Taurus Crash Pulse

5.2.4 Reverse Seatbelts

A possible countermeasure for far-side impacts is the use of a reverse 3-point seatbelt. A traditional seatbelt starts at the driver's outside shoulder, latches at the inside waist, and ends at the outside waist. A reverse belt is just the opposite – inside shoulder to outside waist to inside waist. The rationale behind this setup is to utilize the inside shoulder belt to prevent occupant excursion. Injuries occurring from far-side impacts stem from the occupant sliding out of the shoulder belt and moving to the passenger seat. The reverse belt will capture the shoulder neck region and possibly keep the occupant in its seat.

Modeling the reverse belt involved reflecting all seatbelt anchors and the retractor mechanism about the centerline of the seat. The y-axis coordinates of the nodes for the lap and shoulder belts were also reflected about the centerline of the seat. However, by doing this, the normal for each facet reversed and needed to be reflected back towards the occupant.

5.2.5 Airbags

In addition to the reverse belt, some further countermeasures included inboard chest and shoulder airbags. Ellipsoids were used to roughly simulate these. Figure 4 below shows the location and size of these ellipsoids. A soft function with high hysteresis was chosen to represent the airbag for simplicity.

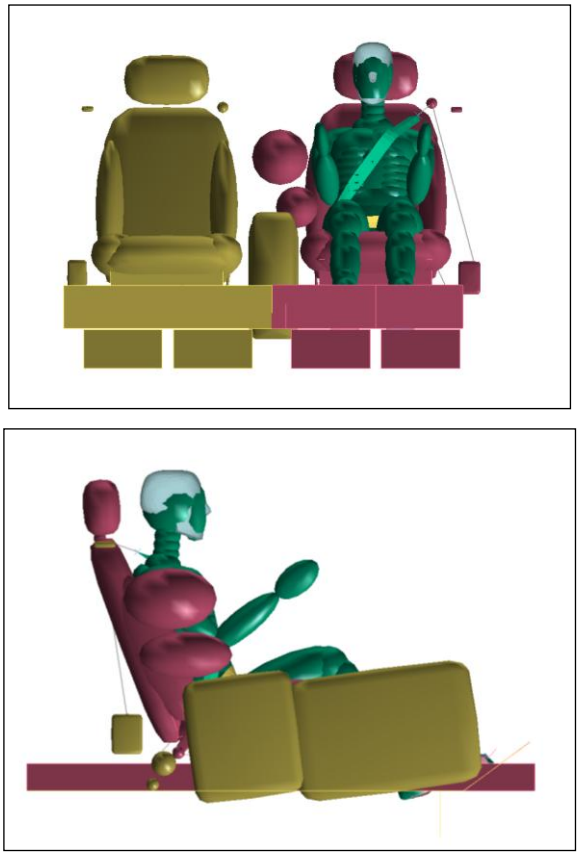

Figure 4: Airbag locations

5.2.6 Test Matrix Summary

Six dummy models in total were analyzed, they were,

1. Hybrid III
2. BioSID
3. EuroSID I
4. EuroSID II
5. SID2s

With these models, five vehicle configurations were simulated –

1. Baseline (just vehicle interior)
2. Reverse Belts
3. Base with chest airbag
4. Base with shoulder airbag
5. Base with chest and shoulder airbag

All five configurations were repeated again for the six dummies, but with a 45degree crash pulse. This totaled 50 simulations for the dummies, excluding human models.

5.3 Results

5.3.1 Evaluation of Countermeasures by Each Dummy Model

The 50 simulations were completed and animations analyzed for correctness. Any bugs in the simulations were addressed and removed. Each simulation outputted an animation accompanied with time history plots of predefined measurements for certain properties, such as forces and accelerations.

The following discussion is limited to modeling and simulation of the 5 anthropomorphic test devices (ATDs). The results of the human finite-element model and human faceted model are unique and require separate discussion.

5.3.1.1 Baseline

For all 5 ATDs in the baseline configuration with 90 degree side-impact pulses, the restrained dummy moved towards the centerline of the vehicle. After translating, the hips of the dummy struck the center console while the upper body continued to move towards the far-side. The pelvis, restrained by the lap belt, held the dummy's hips into the seat. Meanwhile the upper torso slid out of the shoulder belt and rotated over the center console. The five ATDs grossly performed similarly, with the head of the ATD extending towards the center of the passenger seat while and the upper torso rebounded back to the driver

seat. Some slight differences were seen in the rotation motion of the dummy as a result of various spinal constructions.

Seen in the animations, the highest likelihood of injuries for this case occurred in the neck and head. As the upper body rotated around the center console, the head and neck behaved as a spring-mass system, where the head is a mass on top of a spring, the neck. The head pulled and whipped the neck as motion was displayed. The head failed to make contact with any hard surfaces.

Figure 5 charts each dummy's prediction of neck injury. Three metrics were used – F_z, neck tension and compression; F_y, neck shear force; and M_x, the bending moment about x-axis. All these measurements were taken at the upper and lower bodies of the neck. The graphs display the peak forces and moments for each measurement.

The vertical axis represents the percent value of the injury assessment reference value (IARV). A chart of IARV's used is shown below.

Upper Neck		IARV	IRV (Research Only)
+/- Fx	fore/aft shear	3100	
+/- Fy	tension		3100
+ Fz	compression	3290	
- Fz	lateral shear	4000	
+/- Mx	flexion		134
+ My	extension	190	
- My	lateral bending	77	
+/- Mz	twist		77

Lower Neck		IARV	IRV (Research Only)
+/- Fx	fore/aft shear	3100	
+/- Fy	tension		3100
+ Fz	compression	3290	
- Fz	lateral shear	4000	
+/- Mx	flexion		267
+ My	extension	380	
- My	lateral bending	154	
+/- Mz	twist		77

Chart 1: Injury Assessment Research Values

5.3.1.2 Chest Bag

By using the chest airbag, the occupant initially translated toward the centerline of the vehicle. Once the pelvis, struck the center console, the upper torso began rotating until the chest airbag made contact with the ribs. Rib compression was seen and the shoulders rotated slightly around the chest airbag. Occupant excursion wasn't nearly as far as baseline cases, however, whipping of the head and neck was still seen.

The SID2s stuck the chest bag with its shoulder, instead of rib cage. This is a result of the small stature of this dummy.

Neck measurement numbers while using the chest airbag are also shown in figure 5.

5.3.1.3 Shoulder Bag

The shoulder bag restrained the upper torso of each dummy from rotating around the center console. However, each dummy reacted differently as a result of different shoulder construction. The SID2s struck the shoulder bag with its neck. Neck data for all dummies is in figure 5.

5.3.1.4 Chest and Shoulder Bags

With results very similar to just the shoulder bag, the chest and shoulder bags together restrained the dummy from rotation around the center console. The result was an upper torso with very little motion and an unrestrained head whipping around. Data is in figure 6.

5.3.1.5 Reverse Belts

The reverse 3-pt belt system restrained the dummy by the neck from rotated around the center console, preventing occupant excursion. However, resulting neck loads were significantly increased. The BioSID data was excluded due to instabilities in the model that could not be resolved.

5.3.2 Human Finite Element Model

The human finite element was unable to run until completion due to mathematical instabilities, which were insurmountable. In the baseline setup, as with the other dummy models, the human translated toward the centerline of the vehicle. The hips of the dummy initially made contact with the center console and the pelvic area started to deform. At this point, the dummies' upper bodies rotated around the center console. Unlike the dummies, the human continued to translate until the center console intruded far into the pelvic region. It was here that the model would go instable due to the large deformations and displacements.

In the cases of chest and shoulder bags, the airbags intruded the human in the ribs and shoulder respectively. Again causing large deformations and the model went unstable. When the human moved into the airbags very little rotation was observed.

5.3.3 Human Faceted Model

The human faceted model, although experimental, showed the most similar results to the PMHS head strike observation. The human would translate into the center console and continue translating while rotating until the head reached the opposite side of the vehicle.

The chest and shoulder airbags effectively restrained the human into its seat. The results from this model were purely visual. The numerical outputs were more difficult to interpret and compare evenly with the ATDs. Therefore, the results for both human models are limited to visual observations.

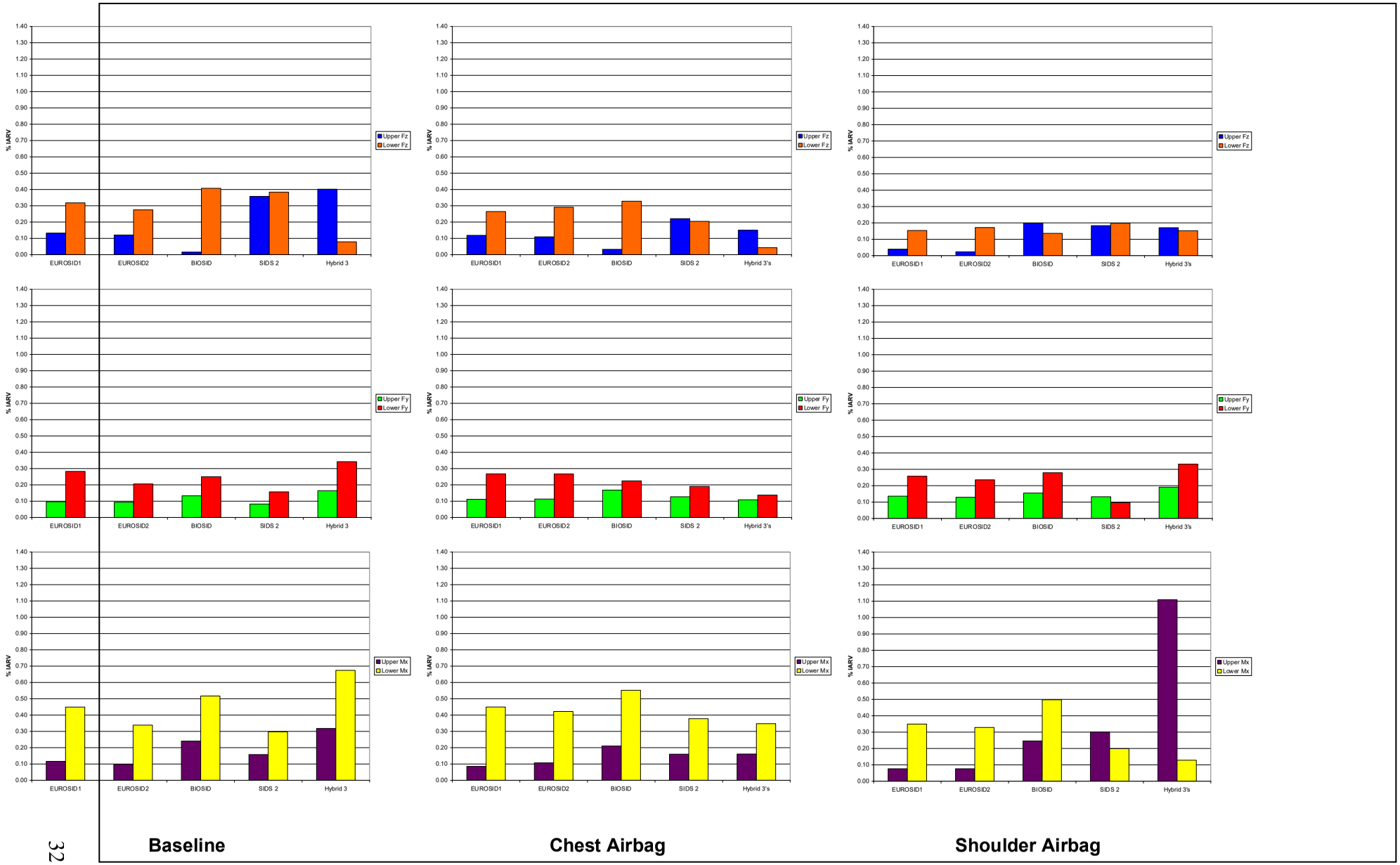

Figure 5: Neck Output

5.4 Discussion

For each of the simulations shown in the current base configuration without use of countermeasures, it was seen that occupant excursion existed towards the passenger seat, but did not reach the door. Although the dummies reacted similarly, differences still existed. For example, the BioSID, with a rigid spine was not able to bend easily around the center console, transmitting more load into the neck. Conversely, the Hybrid III with the exact same neck contained lower forces. The flexible spine of the Hybrid III allowed it to bend and thus decrease neck forces.

For all baseline simulations with the five dummies, injury prediction levels were below accepted injury threshold. Despite the amount of motion observed, there was little to cause injury.

Contrary to these results, it is known that far-side vehicle impacts cause a high number of fatal head injuries annually. Fildes, Sparke, et al. showed that a post mortem human subject's (PMHS) head can strike the B-pillar in far-side impacts. In none of the simulations, did the simulated dummy make contact with any surface inside the vehicle. This is similarly confirmed by Fildes, Sparke, et al. by testing a BioSID, EuroSID 1, and WorldSID in comparable circumstances. None of the dummies tested struck the B-pillar. The MADYMO simulations included BioSID and EuroSID1 in addition to three other dummies with similar results.

Further, to assess the dummies' suitability for far-side testing, countermeasures were introduced to prevent occupant excursion and test the dummy reaction. They were chest and shoulder airbags and a 3-point seatbelt in reverse direction. Each limited occupant excursion, however, exposed more unique possibilities of injuries.

A chest airbag prevented some excursion, but not nearly as much as the shoulder bag or reverse belt. However, it restrained each dummy in the rib region, which introduces the potential for rib injuries.

The shoulder airbag restrained each dummy at the top of the torso. This was effective at preventing occupant excursion, however, left the head unrestrained. By restraining the upper body and leaving the head unrestrained put additional load on the neck, which the Hybrid III demonstrated was close to injury value, but still below the injury threshold.

The chest and shoulder bags together acted similarly to the shoulder bag alone. This situation looked much like a near-side impact and contact with a door. Again, the head is unrestrained and put additional stress on the neck.

The SID2s was the only odd sized dummy used. The EuroSID I and II, BioSID, and Hybrid III are all based on a 50^{th} percentile male. The SID2s, based on an adolescent, exposed vulnerability of the chest and shoulder bags to odd sized occupants. The SID2s struck the chest bag with its shoulder and the shoulder bag with its head/neck. Positioning of these bags can be difficult for oversize and undersized occupants.

Additionally, the chest and shoulder bags showed possible weaknesses of the countermeasures for elderly occupants with weak bones. The chest bag put nearly all forces into the rib areas, and the shoulder bag onto bones of the shoulder.

The reverse 3-point belt is a very simple and cheap method for an automaker to restrain an occupant for far-side collisions. The simulations demonstrated the effectiveness of such a countermeasure. All ATDs were prevented from moving over the center console, by grabbing the neck. Although effective at restraining motion using the neck, this sensitive area of the body can lead to further injuries. MADYMO was able to show significantly higher neck load forces for this situation, many beyond injury thresholds.

For an assessment of countermeasure effectiveness, the individual results of the five dummies were averaged together for every configuration. Figure 7 shows the neck loads of the dummies combined. The near injury threshold of the reverse belts can be seen. For all other airbag countermeasures, all neck loads fall far below injury thresholds and difficult to distinguish among one another.

5.5 Conclusions

Side-impact dummies, designed primarily to test for occupant injuries on the near-side are limited in their ability to emulate occupant kinematics for a far-side impact. Also a Hybrid III test device, designed primarily for frontal impacts, is limited in its ability to test for far-side impacts. Based on historical crash data, the leading cause of injury in side-impacts on the far-side is head strikes with the opposite side hard vehicle surfaces. The occupant kinematics that led to this result were reproduced with a post mortem human subject (PMHS). The cadaver, seated in the vehicle, moved out of its seat and contacted the far-side B-pillar when its vehicle was impacted on the far-side.

Computer simulations offer an easy way to test additional dummies and circumstances. Five anthropomorphic test devices (ATDs) were simulated in MADYMO for far-side impacts and all reacted similarly to the three dummies tested previously as would be expected, and failed to produce desired kinematics.

Despite the short-comings of the dummies for reproducing far-side kinematics, the reaction of these dummies in MADYMO to certain countermeasures offers some insight into future studies. A reverse 3-point seatbelt effectively restrained the occupant, however, significantly increased neck force levels, almost crossing injury threshold levels. Chest and shoulder airbags on the inside of the occupant contained the occupant and prevented excursion. However, left the head and neck unrestrained and showed awkward movement of the head. In addition, the use of a petite dummy exposed some vulnerability of odd sized occupants to airbags.

The human faceted MADYMO model did show promise by properly reproducing occupant kinematics. Future simulations and experimentation are necessary to determine whether such a model could appropriately predict occupant injury and kinematics for far-side impacts. In addition, a modified BioSID dummy tested by Bostrom properly contacted the far-side B-pillar and could be modeled for suitability.

5.6 References

Bostrom, O., Haland, Y., (2004) Benefits of a 3+2 Point Belt System and an Inboard Torso Side Support in Frontal, Far-Side, and Rollover Crashes.

Cavanaugh, J.M., Zhu, Y., Huang, Y., King, A.I. (1993) Injury and Response of the Thorax in Side Impact Cadaveric Tests. SAE Paper 933127.

Fildes, B.N., Sparke, L.J., Bostrom, O., Pintar, F., Yoganandan, N., Morris, A.P. (2002) Suitability of Current Side Impact Test Dummies in Far-Side Impacts. IRCOBI Conference. September 2002.

Maltese, M.R., Eppinger, R.H., Rhule, H., Donnelly, B., Pintar, F.A., Yoganandan, N. (2002) Response Corridors of Human Surrogates in Lateral Impacts. Stapp Car Crash Journal, Vol. 46, Society of Automotive Engineers, Warrendale, PA.

Yoganandan, N., Pintar, F.A., Gennarelli, T.A., Maltese, M.R., Eppinger, R.H. (2002) Biofidelity Evaluation of Recent Side Impact Dummies. IRCOBI Conference. September 2002.

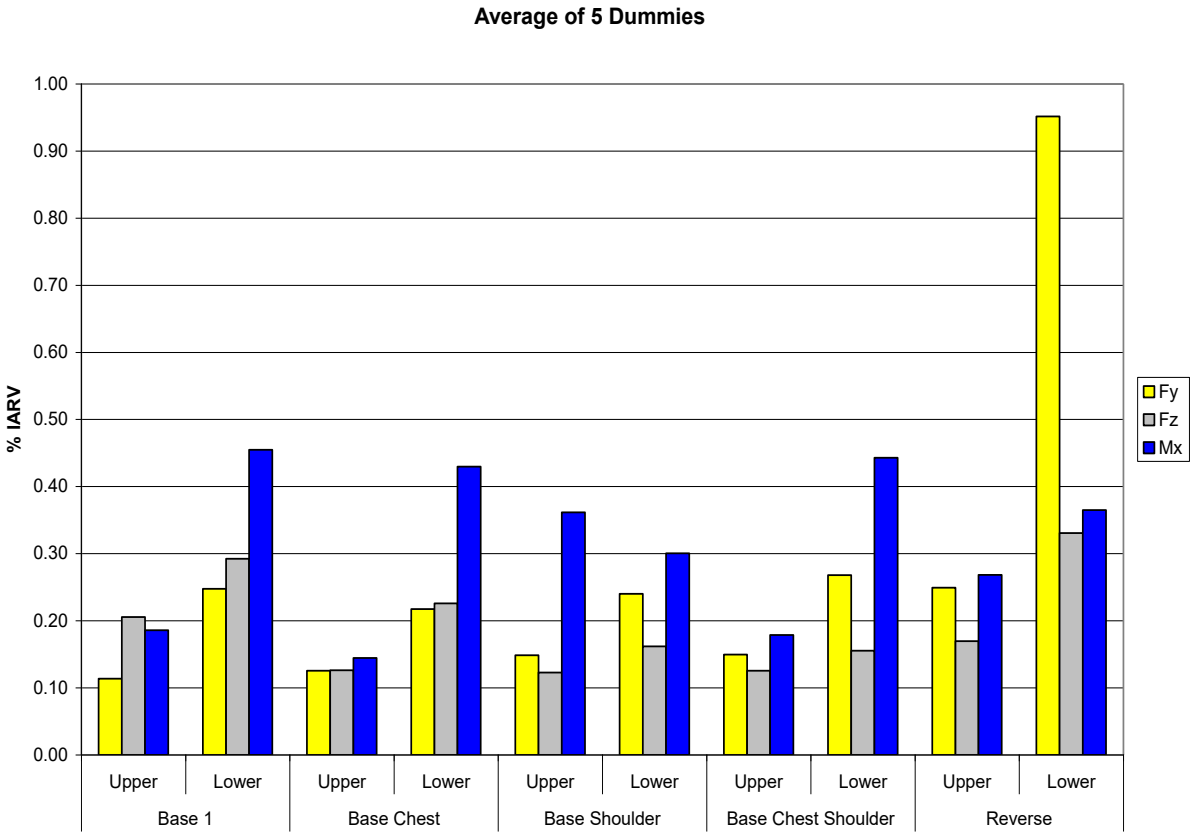

Figure 7: Countermeasure Combined Neck Loads

6 Sled Test Configurations for the Far-Side Crash Environment

6.1 Introduction

This research applies finite element modelling and occupant modelling to determine the sled test conditions required to simulate crash environments that produce significant numbers of AIS 3+ injuries to far-side occupants. Of particular interest are angular crashes and crashes that produce vehicle rotation that could influence occupant kinematics. The SNCAP test was included in the study because the striking barrier's direction of travel is 63 degrees relative to the centerline of the struck vehicle.

The following crash modes were modelled in this study:

- SNCAP Crash Test
- Y Damage Crash Test
- 40% Overlap 30° Corner Impact Crash Test

6.2 Background

The crash environment that produces injuries in far-side impacts has been studied by others [Gabler 2005, Digges 2001]. A large number of crashes that produce serious injuries occur in configurations that produce rotation of the impacted vehicle. To date, the countermeasures being evaluated in sled tests that do not consider the complications created by vehicle rotation [Bostrom 2003]. A requirement exists for appropriate sled test configurations to permit the economical development of effective far-side countermeasures. Initial considerations of the sled test requirements for crashes with rotation have been published by Smyth [2007]. The present study is based on a thesis for a Master's degree at the George Washington University [Cuadrado, 2008]. The thesis contains additional simulations based on finite element models of vehicle-to-vehicle crashes and in-depth evaluations of the requirements for a sled crash pulse.

The change in velocity, or delta-V, is a metric frequently used by researchers and experts to define crash severity and determine injury causation [Palmer 2006]. Numerous studies have analysed the relationships between the vehicle delta-V, occupant delta-V, and occupant injury [Marine 1998, Buhdorf 1996, Roberts 1993]. For cases with negligible vehicle rotation, the occupant delta-V is similar to that of the vehicle [Cheng 1989]. However, the delta-V must be calculated for every position within the vehicle if it rotates to account for the change in angular velocity and angular displacement [Fay 1996]. Taking the rotational component into consideration means that the total delta-V for occupants on one side of the vehicle will be reduced while increasing the total delta-V for occupants on the other side of the vehicle [Fay 1996]. This fact is pertinent in understanding the differences in the crash environment between near and far-side occupants.

Another important consideration is that near-side occupants contact the inside of the vehicle within 50 ms of the initial impact while far-side occupants can strike the interior as late as 180 ms after impact [Solinski 1997]. This is particularly significant in side collisions. Near-side passengers are commonly struck by the intruding interior while far-side occupants have sufficient interior space to permit more of the crash energy to be absorbed by restraint systems before contact with the vehicle interior occurs. In addition, the longer "ride down" time for far-side occupants permits more time for a rotating vehicle to move relative to the occupant. Consequently, the influence of the vehicle's motion and intrusion will be different for far-side occupants.

Automotive manufacturers would be encouraged to develop countermeasures for occupants seated on the non-stuck side of a vehicle if there were sled test procedures to evaluate the safety performance. To date there have been very few crash tests with dummies on the far-side of the crash. The primary purpose of this study is to develop sled tests that mimics the far-side crash environment. The tests selected for this study include the SNCAP test and tests of vehicles that undergo significant yaw during the event. A successful duplication of occupant motion in far-side crashes will prove that a sled test is an effective, cost-efficient means of testing and developing safety countermeasures for far-side occupants.

6.3 Methodology

The kinematics of far-side occupants exposed to impacts that involve vehicle rotation are largely unknown. As of 2007 there are over 5000 crash tests in the National Highway Traffic Safety Administration (NHTSA) database, but only three tests were found to have been performed with a far-side dummy. These tests were unable to be used in this study because they were not instrumented with accelerometers in the lateral direction and poor video quality prevented accurate yaw data to be obtained through video analysis. In addition, US Government research has not conducted crash tests in configurations that are responsible for most of the far-side injuries. Consequently, the far-side occupant motion in a crash test configuration must be determined in order to design a sled test for each considered case. The cases chosen in this study were based on three full-scale crash tests that were available in the GW film library. None of these crash tests contained a dummy on the far-side of the vehicle.

The methodology involved running the MADYMO model in two steps [MADYMO 2004]. The MADYMO human facet model was selected based on the validation of the model for far-side occupant simulations by Alonso [2005].

In the first step, the actual vehicle acceleration and yaw experienced by the subject vehicle in each crash test were used to create the acceleration environment for a MADYMO model to determine the motion that a far-side occupant would undergo in each crash mode. The computer model permits the vehicle to undergo both linear and angular accelerations that vary with time. Consequently the actual rotation of the vehicle can be simulated. However, it is assumed that the sled angle will remain constant. The challenge is to determine the appropriate sled angle to simulate the far-side crash environments represented by injury producing events.

The second step was to determine a sled test with a constant angle of rotation that best simulates the far-side occupant motion and contacts. In this step, runs with different sled angles were conducted and the far-side occupant motion was compared with the response in the crash test from step one.

The input variables of the sled test model were altered until the occupant motion matched that of the crash test model. The reference condition for the evaluation of occupant motion was the occupant restrained only by a lap belt. The objective was to match the trajectory of the head as closely as possible to the occupant in the crash pulse model. The lap belt configuration was chosen to maximize the amount of distance the occupant's head would travel unimpeded. Errors that may be indistinguishable when comparing 3-point belted occupants will be exacerbated due to the longer travel distance. The proper configuration was then simulated and compared for occupants using 3-point belt restraints. The final sled test configuration can then be used in an actual sled test to mimic the occupant motion of a far-side occupant exposed to the original crash environment.

6.4 Vehicle Model Development

The NHWA/NHTSA National Crash Analysis Center's vehicle modelling laboratory has created a library of 14 vehicle finite element models that are available for download and public use. The database contains 3 sedan models, the most detailed of which is a 2001 Ford Taurus. This model was chosen for the MADYMO simulations because all 3 crash tests were performed with sedans. A single vehicle geometry was used to model each pulse in this study in order to isolate the effect that the sled angle has on the occupant motion. This simplification allows for a baseline comparison between crash tests by eliminating differences due to different vehicle interior geometries.

The Taurus model was reduced to the components that would be interacting with the occupant during the tests in order to minimize the simulation time. Once the model was reduced to the necessary components, several preliminary simulations were run and determined that a 200 ms crash simulation would take over two hours to complete. The model was simplified further by using larger elements to capture the interior geometry of the vehicle. This lowered the number of elements from 75675 elements to 4089, thus reducing the simulation time to approximately 7 minutes. The model is shown in Figure 1.

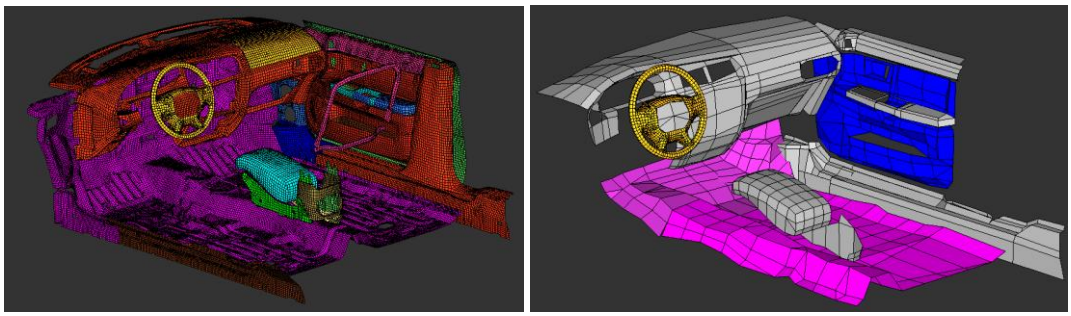

Figure 1. Taurus Cabin Finite Element Model (left) and Reduced MADYMO Taurus Cabin (right)

The dummy model seating position was determined from the 2000 Ford Taurus SNCAP NHTSA Test Report (Test No. 3263). Although more far-side accidents occur with an occupant in the driver seating position, the passenger position was chosen to allow for a greater travel distance before interacting with the vehicle instrument panel.

In this study the sled angle is defined as the angle that the buck is rotated with respect to its position in the crash pulse tests. The pulse is applied to the buck in the negative x-direction of the global coordinate system. The sled angle for a frontal impact test is 0° and is 90° for a side impact test. The initial sled angle for each pulse was set to the impact angle between the bullet vehicle/barrier and the longitudinal axis of the target vehicle. The simulations were then run using the baseline vehicle crash pulse. The sled angle and pulse were then adjusted on a trial and error basis until the timing and contact locations of the sled test occupant matched that of the crash pulse model.

Results from sled test simulations revealed that the angle between the occupant's torso and the instrument panel significantly differed between the crash pulse model and sled test model (see Fig 2). This difference is only noted in crashes where vehicle yaw was a factor. Therefore, the difference was attributed to the rotation of the vehicle relative to the occupant.

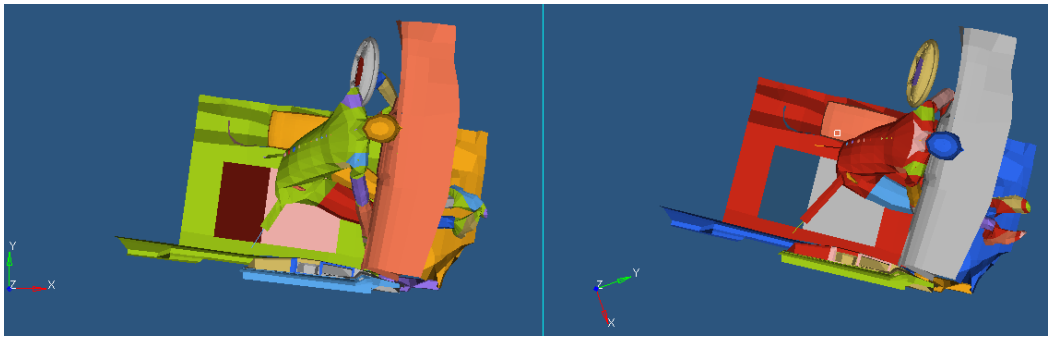

Figure 2. Comparison of 30° Corner Impact Crash Pulse Test (left) to Initial Sled Test (right)

In order to deal with crashes in which the vehicle rotates relative to the occupant, the dashboard on the sled was rotated. This technique created a sled buck with the seat and floorboard in the coordinate system of the crash tests' initial position and an instrument panel in the coordinate system of the crash tests' final position. This sled modification allowed for the vehicle yaw to be considered (see Figure 3).

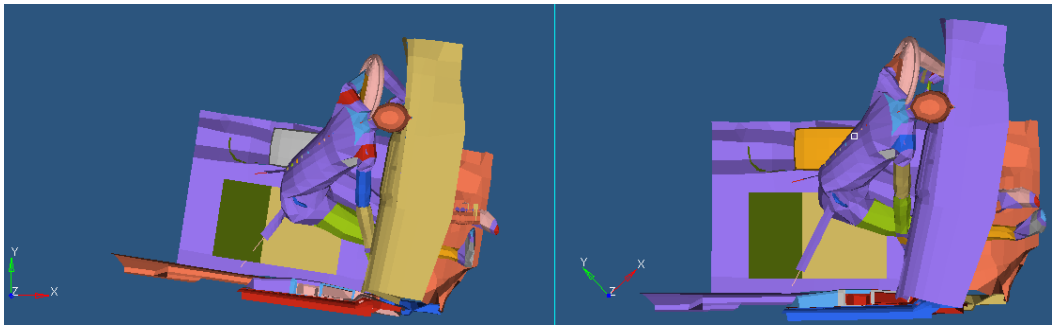

Figure 3. Comparison of 30° Corner Impact Crash Pulse Test (left) to Initial Sled Test (right) with Rotated Instrument Panel

6.5 Simulations

The sled test configurations are defined by the following parameters: pulse shape, pulse magnitude, pulse duration, sled angle, and instrument panel angle. Three crash test cases are presented in detail to demonstrate the process used to determine the proper sled configuration. The cases to follow will concentrate on the appropriate sled angle and instrument panel angle. A discussion of the crash pulses can be found in the documentation for the complete study [Cuadrado 2008].

The available crash tests did not have a dummy located in the far-side seating position. Consequently, the motion of the far-side occupant was simulated using the MADYMO human facet model. The simulation was accomplished by applying the vehicle acceleration pulse measured at the occupant location during the actual crash. This simulation was called "Pulse" because the actual crash pulse was applied to the simulation.

Two belt configurations were simulated. These configurations were lap belt only and conventional three point lap and shoulder belt. In the baseline simulations, the far-side occupant was restrained by a lap belt only. This belt configuration was chosen to provide the most extreme upper body excursion for a restrained occupant. This configuration also represented a worst-case scenario in the event the shoulder belt had no influence on the kinematics.

The kinematics obtained from the lap belt "Pulse" simulations formed the basis for judging the suitability of a sled configuration to provide the same general motion and upper body contact locations. The sled test was simulated applying a constant direction acceleration pulse that was representative of the crash to an occupant compartment configuration that was rotated relative to the direction of travel. The simulations of the sled configurations were labelled "Sled".

It was found that in some crashes, the rotation of the vehicle relative to the occupant was sufficient to require that the dashboard be rotated as well as the sled angle. The kinematics of the far-side occupant restrained by a lap belt was compared with the kinematics from the "Pulse" simulation. The sled and dashboard angles were adjusted until agreement was reached. After agreement of the lap belt configurations, the "Pulse" and "Sled" simulations with three point belts were compared.

6.5.1 NHTSA 4660 30° Corner Impact Simulation

The 30° corner crash test (NHTSA 4660) involved two moving cars that impact in the front corner of the target car. The test was of a 1996 Toyota Avalon impacting a 1997 Honda Accord traveling at 56.6 and 56.2 km/hr, respectively. The target car was impacted at 30 degrees relative to the x-direction centreline. The center of the bullet car impacted the left front corner of the target car. Although this was a frontal crash it involved a side vector that produced significant vehicle rotation. This impact caused the right front passenger to be subjected to far-side acceleration. A right front corner crash is a common far-side crash for the driver of a vehicle impacted while making a left turn across oncoming traffic.

Using the procedure outlined in Sections 2.3 and 2.5, occupant kinematics in the "Pulse" and "Sled" configurations were compared to determine the best sled configuration to simulate the 30 degree corner crash. For this crash configuration the sled test angle was 43 degrees relative to the vehicle y-direction centreline. The vehicle rotation required a dashboard rotation of 8.4 degrees to provide accurate head contact location and timing.

Figures 4-6 show what are considered to be important times in the occupant's motion. Figure 4 shows the initial contact between the occupant's upper body (hand) and the vehicle's instrument panel 60 ms into the simulation.

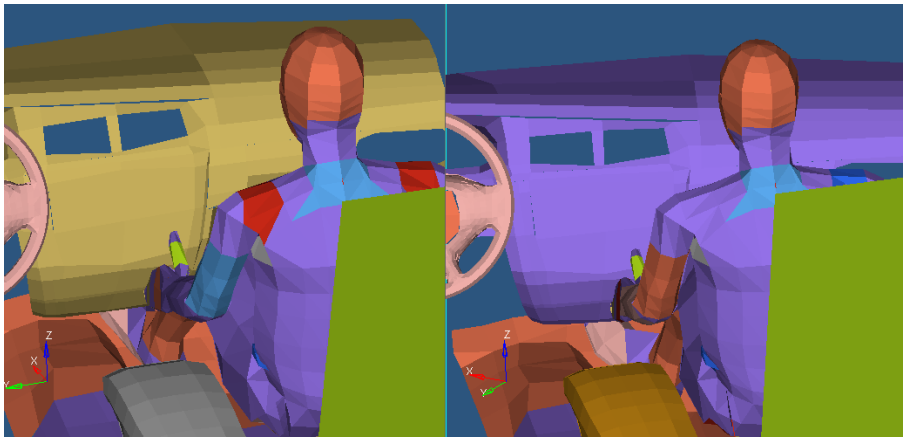

Figure 4. Comparison of Initial Hand Contact at t=60ms Between Crash Pulse Model (left) and Sled Test Model (right)

The most important contact in this analysis is between the instrument panel and the occupant's head or thorax. For this case, the occupant's head contacts the dashboard at approximately 110 ms into the

simulation (Figure 5). The sled test configuration was then run with the occupant restrained in a 3-point belt and the results were shown to match that of the 3-point belt crash pulse test (Figure 6).

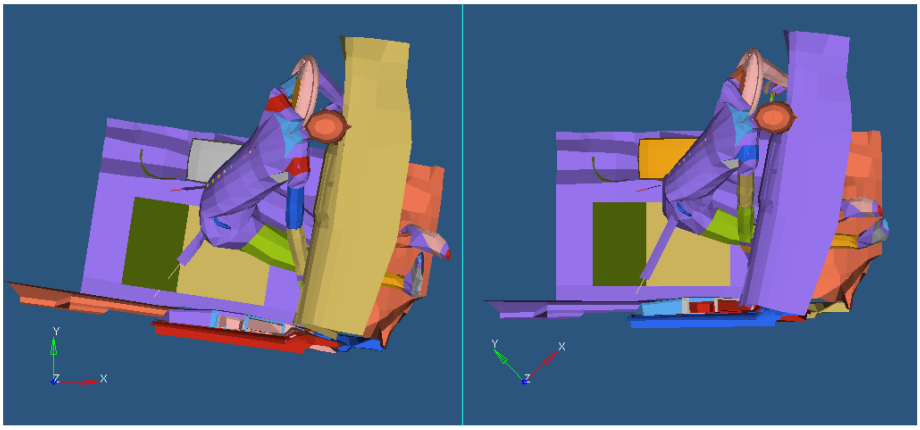

Figure 5. Aerial View at t=110ms between 3-Point Belt Crash Pulse Model (left) and Lap Belt Sled Test Model (right)

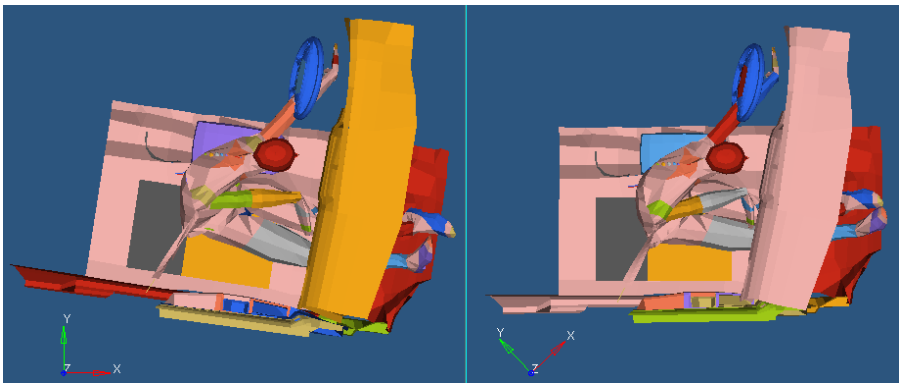

Figure 6. Aerial View at t=110ms between 3-Point Belt Crash Pulse Model (left) and 3-Point Belt Sled Test Model (right)

After completing the visual analysis of the occupant kinematics, the motion of the head was plotted in the coordinate system of the instrument panel. Figure 7 shows that the resultant head excursion for both the lap and 3-point belt sled tests is almost identical to crash test models.

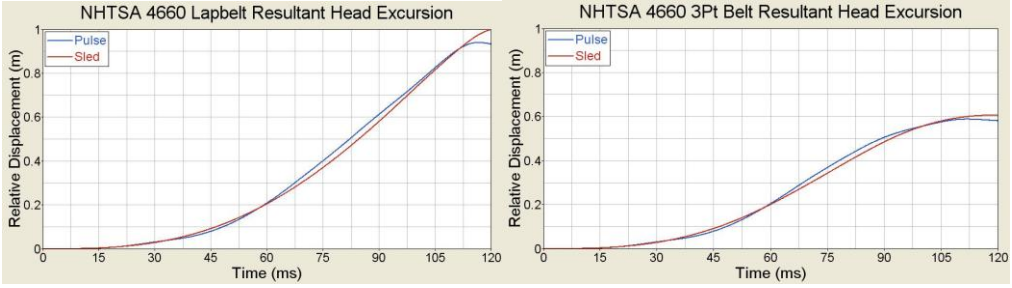

Figure 7. NHTSA 4660 Resultant Head Excursion

Figure 8 shows the PDOF of the occupant's head in the horizontal plane. The pulse models exhibit an overall rotation of approximately 25 degrees.

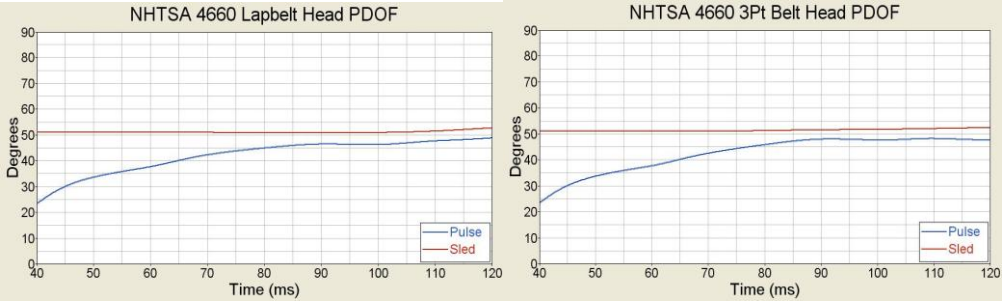

Figure 8. NHTSA 4660 Head PDOF

6.5.2 Y Damage Crash Simulations

This section presents simulation results for occupant's interaction with the vehicle interior for a crash with Y damage based on Collision Damage Classification (CDC) method of accounting [SAE J224]. This classification requires the damage to the vehicle extend over both the center and the front part of the vehicle's side. The test condition for the Y damage case was an S-10 pickup travelling at 30 mph impacting the side of a Ford Taurus at 90 degrees. The center of impact was near the front axle. The longitudinal damage produced was over the forward 2/3 of the side and it was rated Y damage according to the CDC scale.

Using the procedure outlined in Sections 2.3 and 2.5, occupant kinematics in the "Pulse" and "Sled" configurations were compared to determine the best sled configuration to simulate the 30 degree corner crash. For this crash condition, the best sled angle was 87 degrees. The dashboard rotation was 8.4 degrees.

Figure 9 displays the contact between the occupant and center console 75 ms into the simulation. At this point the occupant begins to cross over the vehicle centerline and is in a similar position in both simulations.

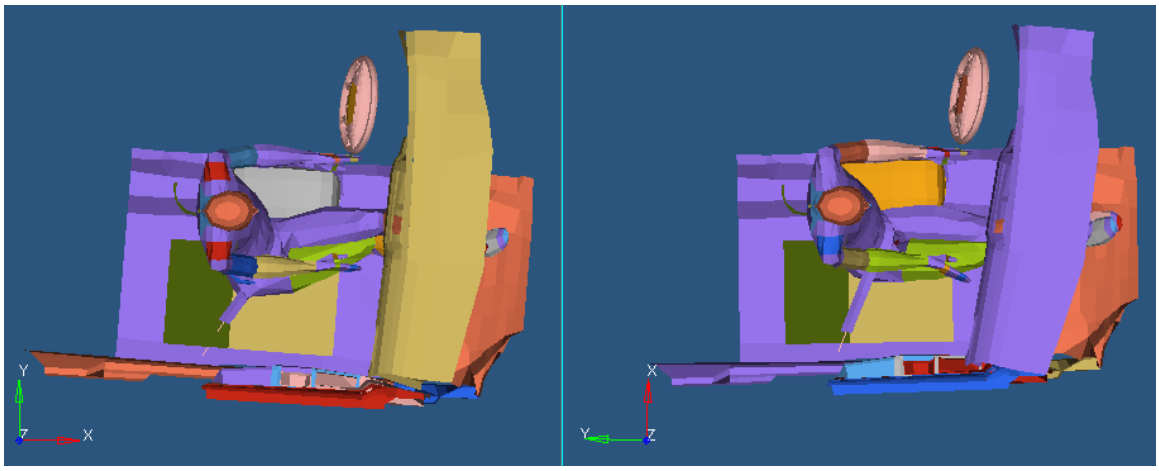

Figure 9. Aerial View at t=75ms between Lap Belt Crash Pulse Model (left) and Lap Belt Sled Test Model (right)

The occupant does not contact the instrument panel in the Y damage test. For this case, the event is considered over when the occupant's thorax began to cross the centerline of the near-side occupant's seat at approximately 110 ms into the simulation (Figure 10). A comparison of the occupant's position relative to the rotated instrument panel shows a similar response in each simulation. This reiterates the significance of rotating the instrument panel in high yaw crashes, as the relative position to the vehicle floorboard is considerably different in each test.

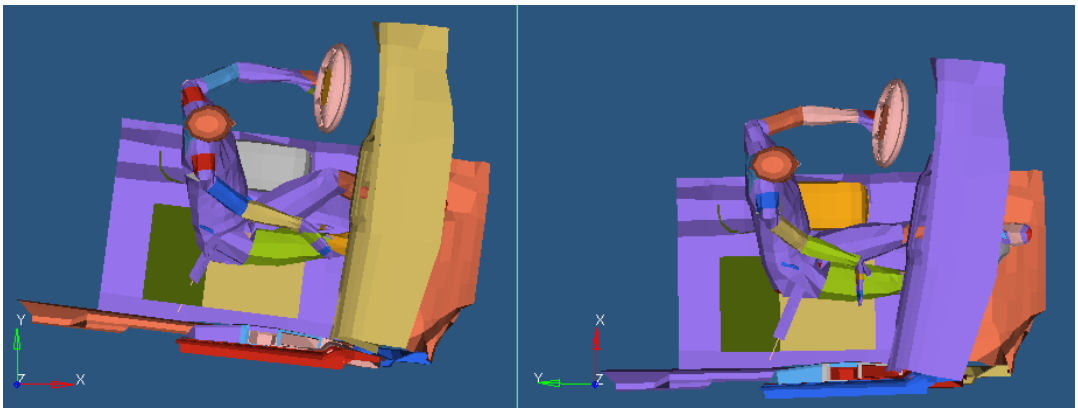

Figure 10. Aerial View at t=110ms between Lap Belt Crash Pulse Model (left) and Lap Belt Sled Test Model (right)

Figures 11 and 12 give frontal and rear views of the crash pulse model and sled test model at 110 ms into the simulation. The slight difference in the models is attributed to the rotation of the crash pulse model. This is most evident in the contact between the occupant and seat observed in (Figure 12). Overall, there is little difference between the contact location and time between each simulation.

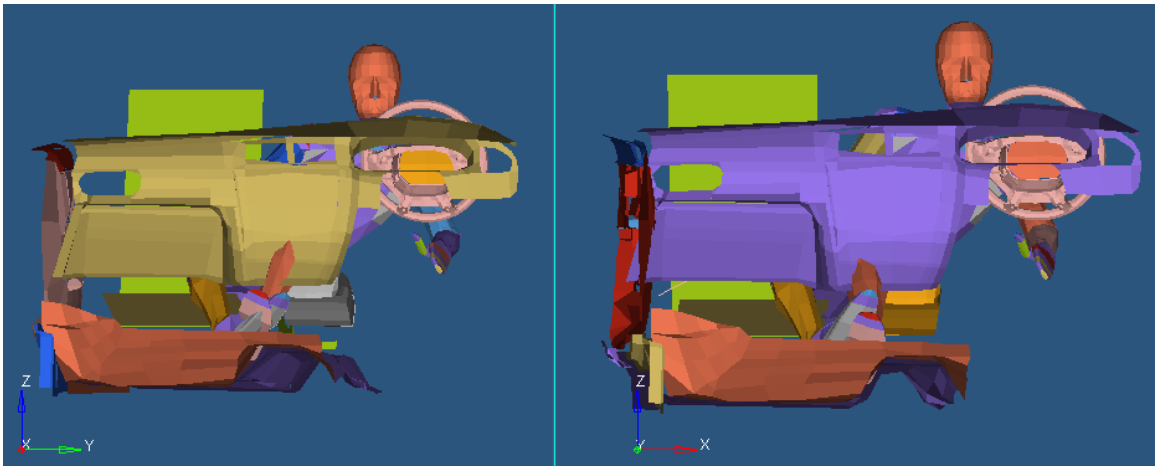

Figure 11. Front View at t=110ms between Lap Belt Crash Pulse Model (left) and Lap Belt Sled Test Model (right)

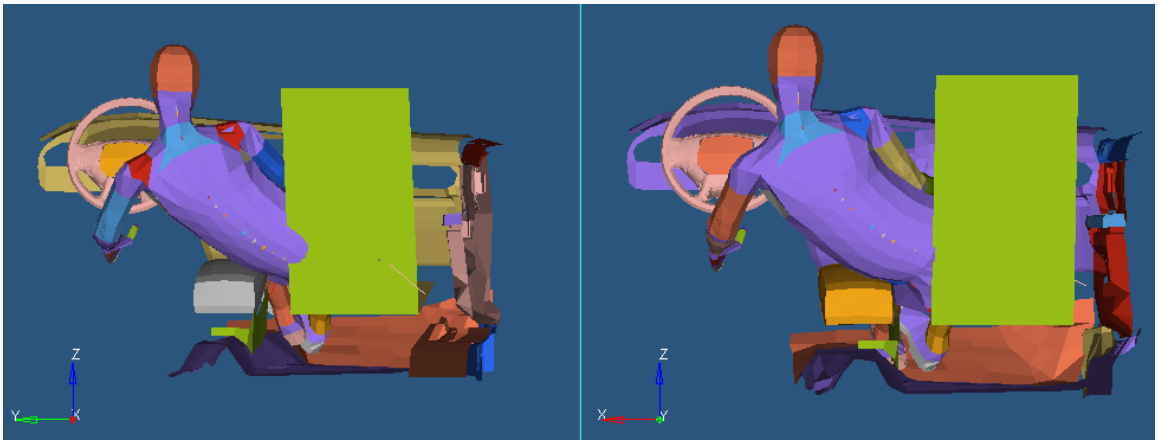

Figure 12. Rear View at t=110ms between Lap Belt Crash Pulse Model (left) and Lap Belt Sled Test Model (right)

The Y damage simulations were run with the occupant restrained in a 3-point belt (Figures 13 and 14). The results of these simulations indicate that the sled test accurately duplicates the motion of the crash pulse model using the same configuration as the lap belt sled test. The simulations show that the occupant slips out of the shoulder belt in this crash environment.

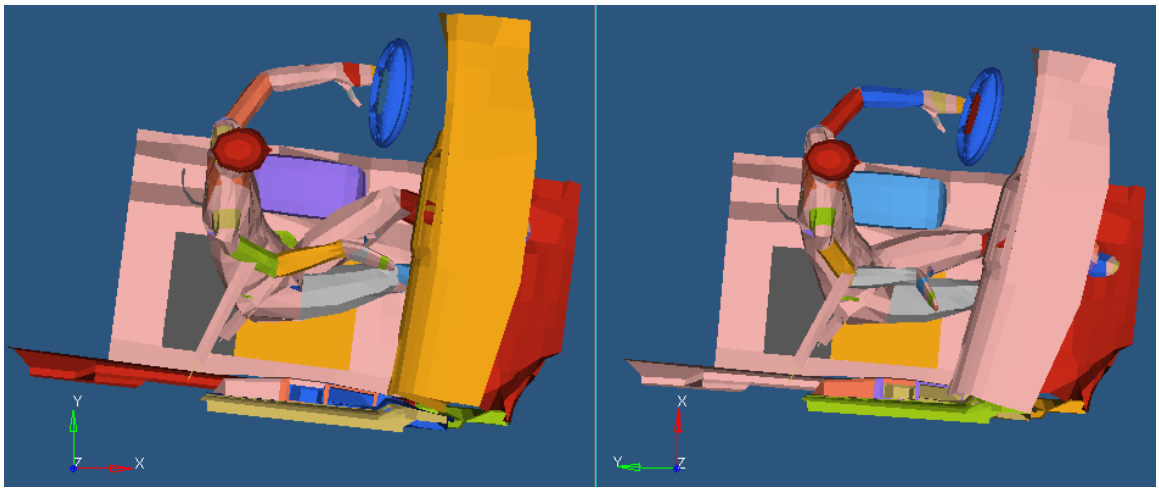

Figure 13. Aerial View at t=110ms between 3-Point Belt Crash Pulse Model (left) and 3-Point Belt Sled Test Model (right)

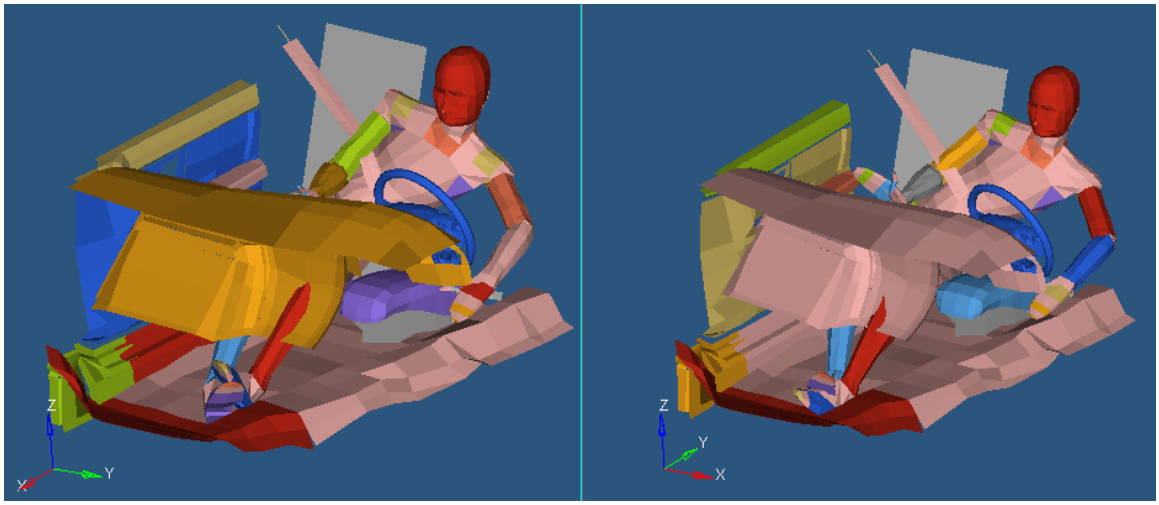

Figure 14. Isometric View at t=110ms between 3-Point Belt Crash Pulse Model (left) and 3-Point Belt Sled Test Model (right)

The motion of the Y damage occupant's head was measured in the coordinate system of the rotated instrument panel (Figure 15). The resultant head excursion for both the lap and 3-point belt sled tests is almost identical to their respective crash test models. The maximum occupant head excursion for the lap belt tests and 3-point belt test were approximately 800 mm and 650 mm, respectively. Although the shoulder belt reduced occupant excursion, the occupant still slipped out of the shoulder belt and crossed into the area that a near-side occupant would be seated.

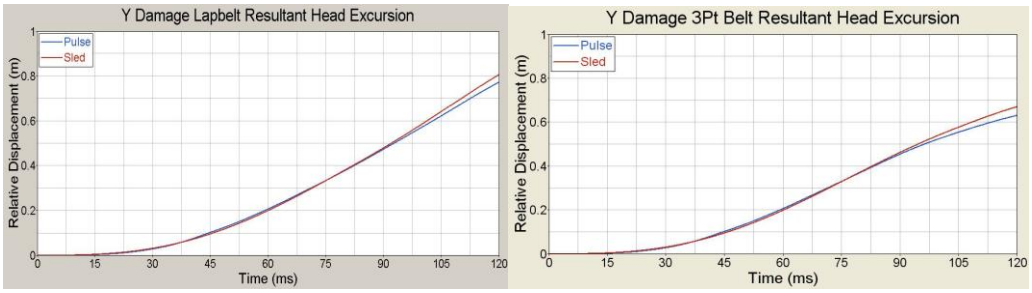

Figure 15. Y Damage Resultant Head Excursion

The accuracy of each sled test can also be seen in the occupant's head PDOF for each case (Figure 16). In each case the final head PDOF is similar between the sled test and crash pulse test, but the lap belted final PDOF is identical between the crash pulse and sled tests whereas the 3-point belt sled test is approximately 5 degrees different from its corresponding crash pulse test. The final head PDOF in all cases is approximately 85 degrees.

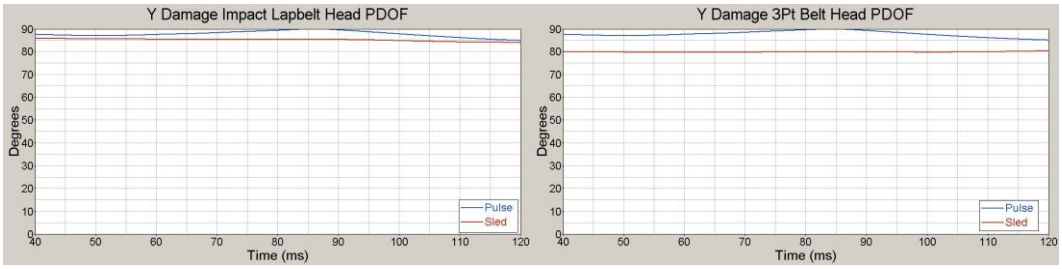

Figure 16. Y Damage Head PDOF

6.5.3 SNCAP Crash Simulations

The SNCAP was chosen for the detailed study because it is based on an actual test performed by NHTSA (Test No. 3263) and it involves an angled crash vector. The test impacted a 2000 Ford Taurus with a NHTSA moving deformable barrier (MDB) travelling at 38.5 mph. The surface of the MDB impacts the vehicle side squarely but has an impact angle of 63° due to the 27° crab angle shown in the figure below. This technique is used to create a longitudinal component in the crash pulse.

Although the travel angle of the movable barrier was 63 degrees, the appropriate sled angle was found to be 87 degrees. No dashboard rotation was required.

The following figures show significant times in the SNCAP occupant's motion. Each occupant in the lap belt simulations (Figure 17) initially contacts the center console 52 ms after impact. The relative position of the occupant within the vehicle is observed to be the same for both simulations.

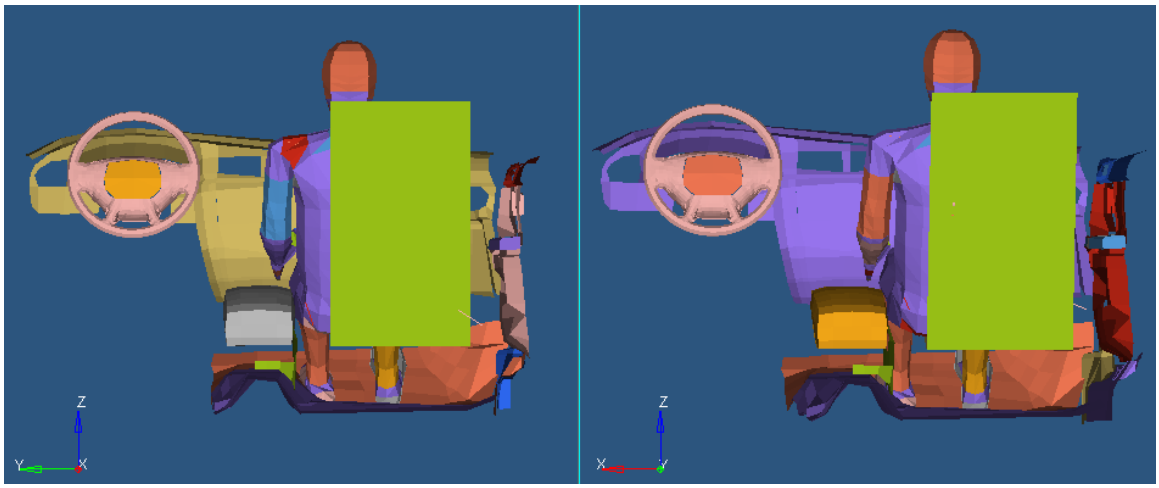

Figure 17. Rear View Comparison of Initial Contact with Center Console at t=52ms Between Crash Pulse Model (left) and Sled Test Model (right)

The motion remains similar up to the point that the occupant crossed the mid-plane of the vehicle. At that point there is significant interaction between the occupant and center console and the crash is considered complete for the purposes of replicating the occupant's motion. The results at this time are shown in Figures 18 and 19.

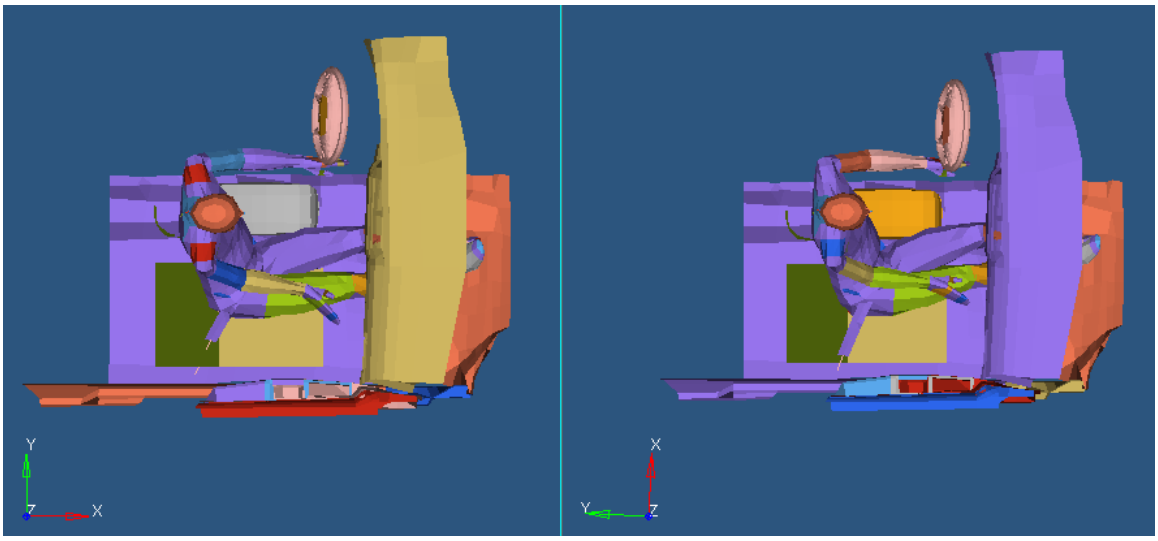

Figure 18. Aerial View Comparison of Occupant Interaction with Center Console at t=90ms between Lap Belt Crash Pulse Model (left) and Lap Belt Sled Test Model (right)

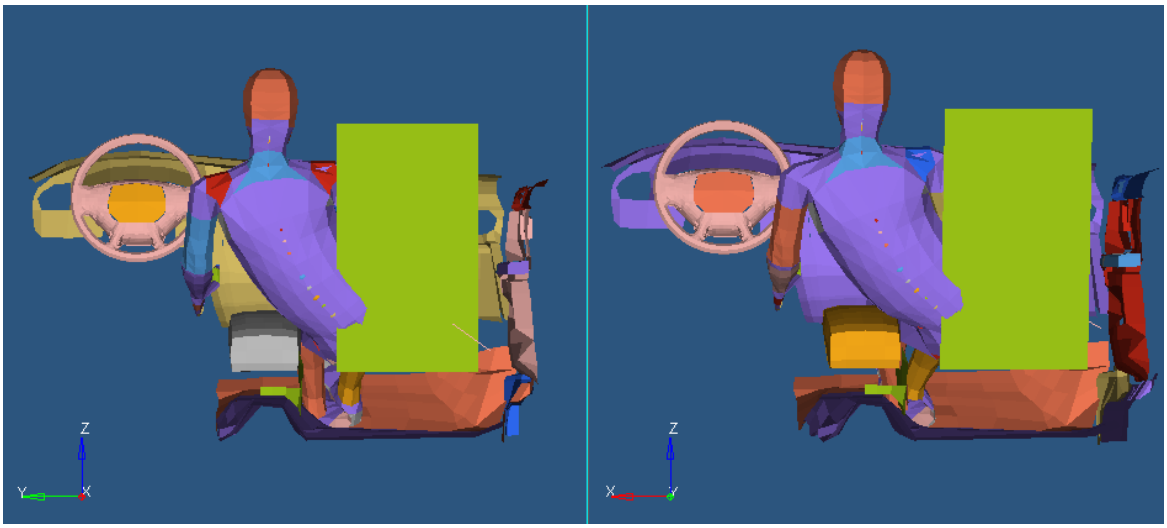

Figure 19. Rear View Comparison of Occupant Interaction with Center Console at t=90ms between Lap Belt Crash Pulse Model (left) and Lap Belt Sled Test Model (right)

The same sled configuration was then run with the occupant restrained in a 3-point belt and the results were compared to the 3-point belt crash pulse test. As predicted, the sled test occupant's motion matched that of the crash test occupant and did not need adjusting with regard to the sled angle or pulse. Figures 20 and 21 indicate that the shoulder belt is ineffective in reducing significant occupant excursion for this crash environment.

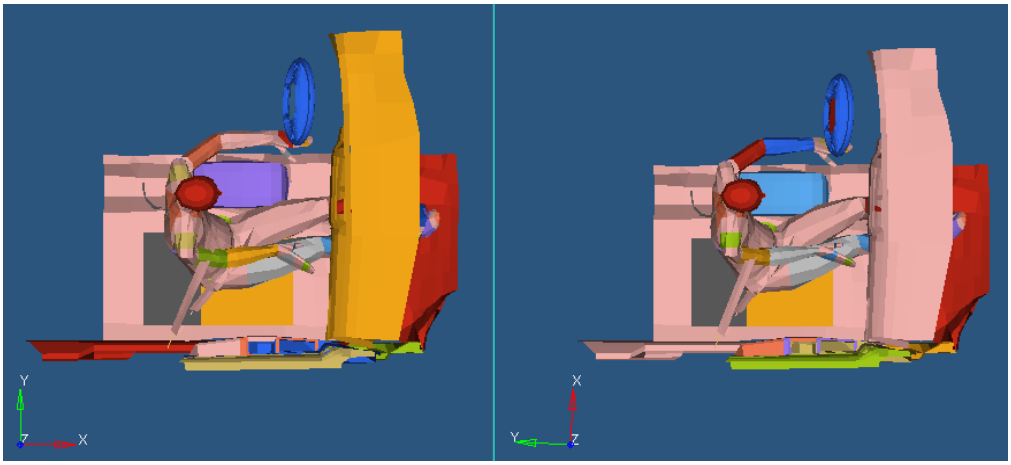

Figure 20. Aerial View Comparison of Occupant Interaction with Center Console at t=90ms between 3-Point Belt Crash Pulse Model (left) and 3-Point Belt Sled Test Model (right)

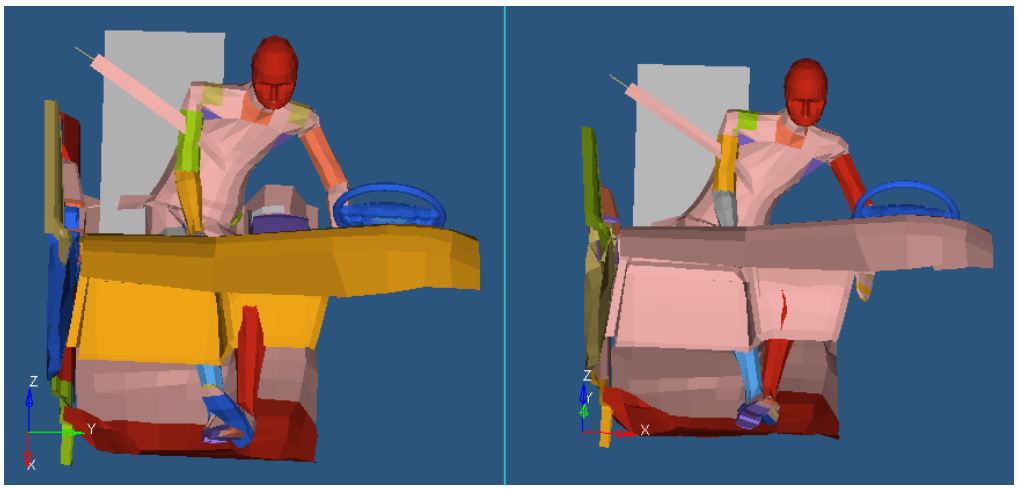

Figure 21. Rear View Comparison of Occupant Interaction with Center Console at t=90ms between 3-Point Belt Crash Pulse Model (left) and 3-Point Belt Sled Test Model (right)

The motion of the occupant's head is shown graphically in Figures 22 and 23. Comparing the results of the occupant only restrained by a lap belt shows that the head excursion is nearly identical for the crash pulse model and the sled test model until about 90 ms after impact. Likewise, the sled test occupant restrained by the 3-point belt had a similar head excursion to that of the crash test. The 3-point belt reduced occupant head excursion by approximately 120 mm, but the resultant head excursion exceeded 500 mm for each test and restraint condition.

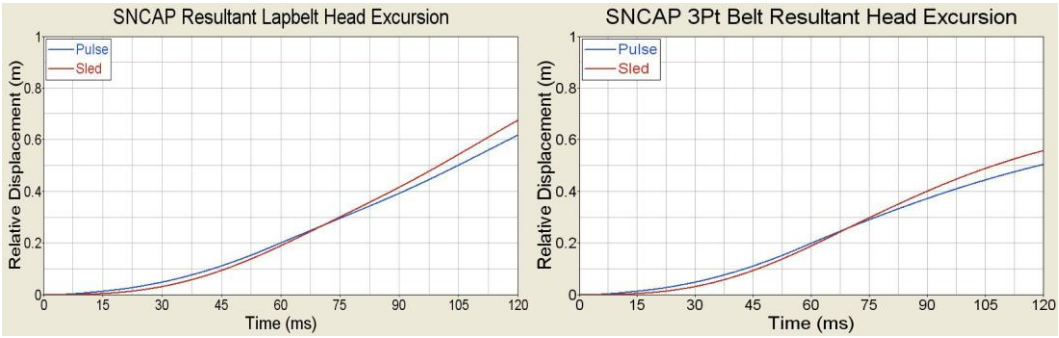

Figure 22. SNCAP Resultant Occupant Head Excursion

The similarities between model response can also be seen in a cross plot of the occupant head excursion in the x/y plane. For this analysis the positive x-direction is in the direction that the passenger is facing when seated in the vehicle. Figure 23 shows that the motion of the occupant's head in the horizontal plane is nearly identical between the crash test and sled test for each restraint design.

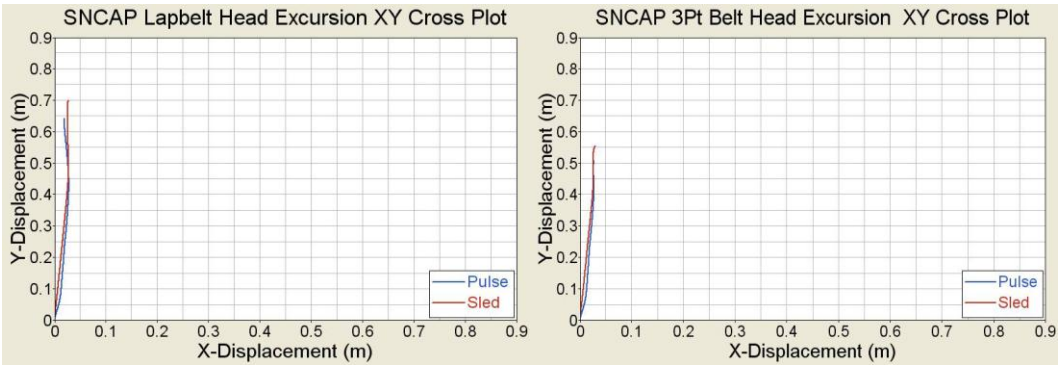

Figure 23. SNCAP Head Excursion Cross Plot

Another means of displaying the motion of the occupant's head is the head principle direction of force (PDOF). The plot (Figure 24) shows that the motion of the occupant's head in the sled test is linear and approximately equal to the angle of the sled (87°). However, the crash test occupant is not constant because of the acceleration being applied in both the longitudinal and lateral directions. After about 70 milliseconds the head PDOF is equal in both the sled and crash test. Of particular importance is that the head PDOF is equal when the event is considered complete at 90ms.

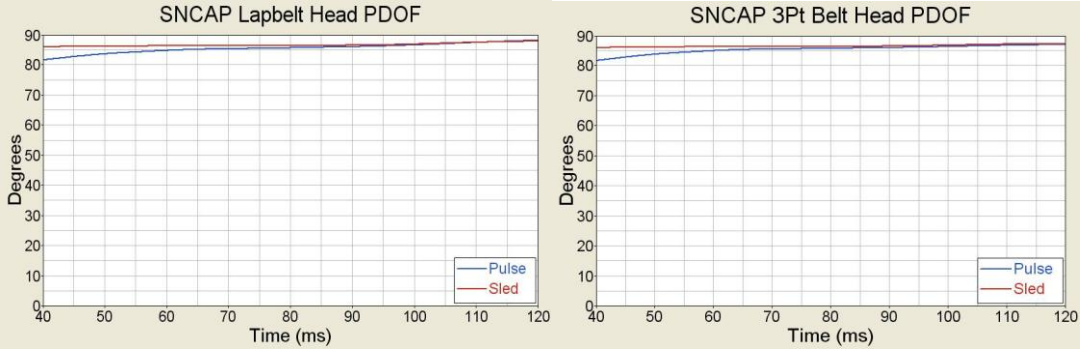

Figure 24. SNCAP Head PDOF

6.6 Simulation Results

Table 1 presents the final sled and instrument panel angle for each test modelled in this study. Although the moving barrier in the SNCAP test had a direction of travel 63 degrees to the struck vehicle centreline, the appropriate sled angle was almost 90 degrees (87º). The Y damage tests had the same sled angle (87°), but required a rotated interior that resulted in the greatest total angle of 95.4°.

Table 1. Summary of Sled and Instrument Panel (IP) Angle

TEST CONFIGURATION	TEST IMPACT ANGLE	SLED ANGLE	IP ANGLE	TOTAL ANGLE
63° SNCAP – 25.8 k/hr	90°	87°	0.0°	87.0°
90° Y Damage ~ 26 k/hr	90°	87°	8.4°	95.4°
30° Corner Impact - 57.6 k/hr	30°	43°	8.5°	51.5°

The instrument panel angle is equal to the vehicle rotation when the event is considered 'over' in each case. For this reason, it is dependent upon the location that the force of impact acts and the moment that it places on the vehicle with respect to the vehicle's center of gravity [7]. This effect is observed by comparing the SNCAP and Y damage tests, which both contact the side of the vehicle. The MDB in the SNCAP test contacts the subject vehicle near its center causing the PDOF to pass near the vehicle center of gravity. The bullet vehicle in the Y damage test contacts the target vehicle in the front of the vehicle creating the 8.4° of rotation observed in the test. It follows that the amount of energy transmitted by the bullet vehicle in a Y damage crash configuration could influence the sled configuration.

The total angle for each test configuration is composed of the sled angle, or angle of the sled buck, and the instrument panel angle, which is equal to the amount of rotation experienced by the vehicle during the event. An increase in the impact angle of the bullet vehicle to the target vehicle typically increases the sled angle, but a direct correlation can not be made between the two angles.

For the three cases simulated, the occupant kinematics of the sled tests accurately mimicked the occupants of their corresponding crash tests. The sled test configuration determined from the lap belt tests was also found to be the proper configuration for occupants wearing 3-point belt restraints.

The accuracy of the sled test occupant excursion is greatly dependent upon the amount of vehicle rotation in the crash test. This is seen in the Head Excursion Cross Plots as the sled tests occupants move in a relatively linear motion while the vehicle rotates underneath the crash tests occupants. The Head PDOF plots reiterate these findings as the Sled curves remains relatively constant and the Pulse curves change dependent on the amount of vehicle rotation. In all cases the Head PDOF of the Sled and Pulse curves are nearly identical when the event is considered 'over' for the crash mode.

6.7 Conclusions

The results from this study show that a sled test can effectively mimic the kinematic response of a far-side occupant in the side and corner impacts for which there was crash test data. The impact angle, initial vehicle velocities, delta-V, and impact location are all important factors in developing a proper sled test configuration. However, no direct correlations were able to be determined between a single variable and the sled pulse or correct sled or instrument panel angle to be used in the test configuration. Of equal importance to each of these variables is how the structure of each vehicle interacts with one another. This interaction is highly dependent upon the previously mentioned variables but can drastically change with small variations in the impact conditions.

Although the results from this study conclude that crashes are too complicated to correlate a single input variable to the sled configuration, certain sled configurations may accurately represent a wide range of

crash environments. For example, a sled test angle of 87 degrees appeared to be appropriate for both the SNCAP and the Y-damage test conditions that were simulated. The use of the approach documented by this paper will provide a basis for determining the best sled configuration to mimic any far-side crash condition.

6.8 References

Alonzo, B., 2005, "Validation of the MADYMO Human Facet Model for Far-Side Crash Simulation", Report to the National Crash Analysis Center, GW University.

Bostrom, O., Fildes, B., Morris, A., Sparke, L., Smith, S., and Judd, R., 2003, "A Cost Effective Far Side Crash Simulation," *UCrash* **8** (3) pp. 307-313.

Bundorf, R., 1996, "Analysis and Calculation of Delta-V from Crash Test Data", SAE Paper No. 960899.

Cheng, P. and Guenther, D., 1989, "Effects of Change in Angular Velocity of a Vehicle on the Change in Velocity Experienced by an Occupant during a Crash Environment and the Localized Delta V Concept," SAE Paper No. 890636.

Cuadrado, J., "Comparison Of Crash Pulses And Sled Responses For Far-Side Impacts", Master's Thesis The George Washington University, March 6, 2008.

Digges, K. and Dalmotas, D., 2001, "Injuries to Restrained Occupants in Far-Side Crashes" *Proceedings of the 17th ESV Conference*.

Fay, R., Raney, A., and Robinette, R., 1996, "The Effect of Vehicle Rotation on the Occupants' Delta V," SAE Paper No. 960649.

Gabler, H., Digges, K., Fildes, B., and, Sparke, L., 2005, "Side Impact Injury Risk for Belted Far Side Passenger Vehicle Occupants," *SAE World Congress*, SAE Paper No. 2005-01-0287.

"MADYMO V6.2 Theory Manual," TNO MADYMO BV, 2004

Marine, M. and Werner, S., 1998, "Delta-V Analysis from Crash Test Data for Vehicles with Post-Impact Yaw Motion," SAE Paper No. 980219.

Palmer, S., 2006, "NHTSA's Final Ruling for Automotive EDRs Will Revolutionize Auto Insurance," Injury Sciences, LLC.

Roberts, V. and Compton, C., 1993, "Relationship Between Delta V and Injury", SAE Paper No. 930311.

Smyth, B and Smith J., 2007, "Developing a Sled Test from Crash Test Data. *SAE World Congress*," SAE Paper No. 2007-01-0711.

Stolinski, R., Grzebieta, R., Fildes, B., Judd, R., Wawrzynczak, J., Gray, I., McGrath, P., and Case, M., 1999, "Response of Far Side Occupants in Car-to-Car Impacts with Standard and Modified Restraint Systems Using H-III and US SID", *International Congress & Exposition*, SAE Paper No. 1999-01-1321.

7 Findings of Studies to Determine Crash and Sled Test Conditions

7.1 Summary of Study Objectives

An objective of this task was to study issues associated with far-side sled testing and crash testing using computer simulation.

Chapter 1 conducted finite element simulations of vehicle and moving barrier crashes into a Ford Taurus. A principal purpose was to determine the degree to which the barriers produced damage patterns that were similar in shape and extent to the vehicle impacts. A secondary purpose was to determine the damage patterns for a frequently occurring crashes at 60 degrees and crashes that impact the front wheels, producing Y-damage.

Chapter 2 conducted MADYMO simulations to determine a dummy or human model that best matched the kinematics of a cadaver that was tested in a far-side crash. A principal purpose was to establish a validated model for use in evaluation occupant response in the far-side crash environment. A second objective was to compare existing dummy models to the cadaver kinematics.

Chapter 3 used the MADYMO human facet model to explore a restraint issue associated with sled testing in far-side crashes. The cadaver test program summarized in Task 2 required a console to provide restraint to the pelvic region. The height of the console should be sufficient to provide pelvic restraint without causing excessive loading of the abdomen. The modeling effort in Chapter 3 explored the occupant kinematics when subjected to consoles of varying heights.

Chapter 4 used the MADYMO human facet model to explore a crash pulse issue associated with sled testing in far-side crashes. The cadaver test program summarized in Task 2 required a crash pulse that was representative of a vehicle-to-vehicle crash. However, the test sled had limited capability to duplicate the highest accelerations that were observed in a crash test. The MADYMO model was used to determine an appropriate sled crash pulse.

Chapter 5 used MADYMO models to explore the interaction between five different dummy models and five different countermeasures. The dummy models were:

1. Hybrid III
2. BioSID
3. EuroSID I
4. EuroSID II
5. SID2s

With these models, five vehicle configurations were simulated:

1. Baseline (just vehicle interior)
2. Reverse Belts
3. Base with chest airbag
4. Base with shoulder airbag
5. Base with chest and shoulder airbag

Chapter 6 used data from crash tests and MADYMO occupant modeling to explore the relationship between the crash PDOF as documented in the accident data and the test sled configuration required to simulate the same far-side crash environment.

Although not part of the far-side project, a complementary series of six crash tests with both near-side and far-side dummies was conducted by The Australian Department of Infrastructure [Newland, 2008]. One purpose of the tests was to examine dummy to dummy interaction.

7.2 Results

The Finite Element Models used in Chapter 1 indicate that the IIHS barrier produced similar damage on a Taurus patterns to those produced by a full size pickup truck. The NHTSA barrier and the Y damage test produced less damage to the Taurus front door than the IIHS barrier.

The average CDC extent of damage produced in actual IIHS crash tests is considerably less that the average extent of damage to vehicles with far-side occupants injured at the AIS 3+ severity. This result suggests that the barrier test speed of a far-side test should be higher than the speed used by IIHS in their side impact tests for consumer ratings.

The MADYMO modeling effort summarized in Chapter 2 found that the human facet model matched the cadaver kinematics very well and it was considered suitable for evaluation of occupant motion in the far-side crash that was simulated. The MADYMO dummy models (Hybrid III, BioSID, EuroSID 1, EuroSID2 and SID2s) did not accurately reflect the motion of a human cadaver under the same impact configurations as the cadaver test.

The conclusion of Chapter 3 was that the force exerted by the occupant on the center console increased as the height of the center console increased. However, when the center console remained low, the belt restraint system restrained the pelvis rather than the center console. As the center console height increased above 8 inches, it loaded the occupant's abdomen and ribs

The modeling documented in Chapter 4 shows that a square wave sled test pulse can produce similar occupant kinematics to the desired car-to-car pulse.

The modeling research reported in Chapter 5 found that side-impact dummies, designed primarily to test for occupant injuries on the near-side are limited in their ability to emulate occupant kinematics for a far-side impact. Also a Hybrid III test device, designed primarily for frontal impacts, is limited in its ability to test for far-side impacts. Five anthropomorphic test devices (ATDs) were simulated in MADYMO for far-side impacts and all failed to produce desired kinematics. However, the human faceted MADYMO model did show promise by properly reproducing occupant kinematics.

Despite the short-comings of the dummies for reproducing far-side kinematics, the reaction of these dummies in MADYMO to certain countermeasures offers some insight into future studies. A reverse 3-point seatbelt effectively restrained the occupant, however, significantly increased neck force levels, almost crossing injury threshold levels. Chest and shoulder airbags on the inside of the occupant contained the occupant and prevented excursion. However, left the head and neck unrestrained and showed awkward movement of the head. In addition, the use of a petite dummy exposed some vulnerability of odd sized occupants to airbags.

The results from this study reported in Chapter 6 show that a sled test can effectively mimic the kinematic response of a far-side occupant in the side and corner impacts for which there was crash test data. It is important to understand that a side impact with a 60 degree PDOF does not translate to a sled test with a sled angle of 60 degrees! For example the SNCAP test has a direction of force of 63 degrees but an appropriate sled angle of 87 degrees. The difference is due to the rapid rotation of the struck vehicle to align with the striking vehicle.

The impact angle, initial vehicle velocities, delta-V, and impact location are all important factors in developing a proper sled test configuration. However, no direct correlations were able to be determined between a single variable and the sled pulse or correct sled or instrument panel angle to be used in the test configuration. The use of the approach documented by this study can provide a basis for determining the best sled configuration to mimic any far-side crash condition.

Tests conducted in Australia have shown that the presence of a far-side dummy does not interfere with the side protection measurements made by the near-side dummy. However, there was interaction between the near-side and far-side dummies during the rebound of the near-side dummy. The interaction occurred well after the far-side dummy slipped out of the shoulder belt [Newland 2008]. These test results indicate that it may be feasible to incorporate a far-side dummy in the vehicles used in consumer information tests. Such a proposal was presented at the ESV meeting in June, 2009 [Digges 2009]. An analysis of safety belt geometry and pretensioning indicates that relatively simple countermeasures can improve far-side protection [Eschemendia 2009].

7.3 References

Digges, K., Echemendia, C., Fildes, B. and Pintar, F.,"A Safety Rating For Far-Side Crashes", Paper Number 09-0217, *Proceedings of the 21st ESV Conference,* June 2009. .

Echemendia, C., "PMHS Far-Side Sled Test Validation with MADYMO", Report to the National Crash Analysis Center, GW University, March 2009. .

Newland, C., Belcher, T., Bostrom, O., Gabler, H., Cha., J., Wong, H., Tylko, S., and Dal Nevo, R., "Occupant-to-Occupant Interaction and Impact Injury Risk in Side Impact Crashes", Stapp Car Crash Journal, Vol 52, pp..327-347, 2008. .